NAVAL POSTGRADUATE SCHOOL
Monterey, California

THESIS

COMPACT CO_2 LASER DESIGN AND ANALYSIS

by

Erik H. Martin

June 1999

Thesis Advisor: D. Scott Davis
Co-Advisor: Robert C. Harney

Approved for public release; distribution is unlimited.

REPORT DOCUMENTATION PAGE

Form Approved OMB No. 0704-0188

1. AGENCY USE ONLY *(Leave blank)*	2. REPORT DATE	3. REPORT TYPE AND DATES COVERED
	June 1999	Master's Thesis

4. TITLE AND SUBTITLE
COMPACT CO_2 LASER DESIGN AND ANALYSIS

5. FUNDING NUMBERS

6. AUTHOR(S)
Martin, Erik H.

7. PERFORMING ORGANIZATION NAME(S) AND ADDRESS(ES)
Naval Postgraduate School
Monterey, CA 93943-5000

8. PERFORMING ORGANIZATION REPORT NUMBER

9. SPONSORING / MONITORING AGENCY NAME(S) AND ADDRESS(ES)

10. SPONSORING / MONITORING AGENCY REPORT NUMBER

11. SUPPLEMENTARY NOTES
The views expressed in this thesis are those of the author and do not reflect the official policy or position of the Department of Defense or the U.S. Government.

12a. DISTRIBUTION / AVAILABILITY STATEMENT
Approved for public release; distribution is unlimited.

12b. DISTRIBUTION CODE

13. ABSTRACT *(maximum 200 words)*

CO_2 lasers, among the most efficient and powerful of all lasers, have many applications in industrial and medical fields. Unfortunately, their typical bulky size and fragility tend to limit their use in austere military environments.

The purpose of this thesis is to present and analyze a new optical cavity design that can possibly fill the need for a compact, high power, ruggedly packaged infrared laser. Such a system could be used for targeting, communications, or field medical use.

The analysis involves entering design parameters into a commercial software program and simulating the behavior of a collimated laser beam within. While results identify significant optical aberration flaws, the extensive design revision needed does not preclude eventual construction.

14. SUBJECT TERMS	15. NUMBER OF PAGES
Carbon Dioxide Lasers, Lasers, Infrared	108
	16. PRICE CODE

17. SECURITY CLASSIFICATION OF REPORT	18. SECURITY CLASSIFICATION OF THIS PAGE	19. SECURITY CLASSIFICATION OF ABSTRACT	20. LIMITATION OF ABSTRACT
Unclassified	Unclassified	Unclassified	UL

NSN 7540-01-280-5500

Standard Form 298 (Rev. 2-89)
Prescribed by ANSI Std. 239-18

Approved for public release; distribution is unlimited

COMPACT CO_2 LASER DESIGN AND ANALYSIS

Erik H. Martin
Lieutenant, United States Navy
B.M.E., Georgia Institute of Technology, 1987

Submitted in partial fulfillment of the
requirements for the degree of

MASTER OF SCIENCE IN APPLIED PHYSICS

from the

NAVAL POSTGRADUATE SCHOOL
June 1999

Author: Erik H. Martin
Erik H. Martin

Approved by: D. S. Davis
D. Scott Davis, Thesis Advisor

Robert C. Harney
Robert C. Harney, Co-Advisor

William B. Maier II
William B. Maier II, Chairman
Department of Physics

ABSTRACT

CO_2 lasers, among the most efficient and powerful of all lasers, have many applications in industrial and medical fields. Unfortunately, their typical bulky size and fragility tend to limit their use in austere military environments.

The purpose of this thesis is to present and analyze a new optical cavity design that can possibly fill the need for a compact, high power, ruggedly packaged infrared laser. Such a system could be used for targeting, communications, or field medical use.

The analysis involves entering design parameters into a commercial software program and simulating the behavior of a collimated laser beam within. While results identify significant optical aberration flaws, the extensive design revision needed does not preclude eventual construction.

TABLE OF CONTENTS

I. INTRODUCTION

A. BACKGROUND AND PURPOSE

It is a difficult intellectual leap for most people to draw any similarity between using a laser for targeting a tank and for cutting denim for blue jeans, yet both are common applications. That is not surprising because, as new technology develops, it frequently takes a foothold in very different environments. The carbon dioxide (CO_2) laser, an invention three decades old, has many diverse diverse industrial applications. This efficient, powerful laser has become a favorite for cutting materials and machining precision parts. Its latest medical applications include resurfacing skin, performing eye surgery, and conducting dental work. However, its military use is severely limited by the bulky structural size and inherent fragility of its conventional optical cavity design.

The effort of this thesis research was to present and to analyze a new design concept for a simple CO_2 laser that involves enhanced specific power and the capability for rugged, compact, modular packaging. See Figure 1-1. The diagram shows the typical CO_2 laser axial cavity, bound by a glass tube, with resonator end mirrors. These come in many sizes; a laser with an output of less than 100 watts is

typically on the order of several feet long by a few inches across. The unit, although capable of substantial output power as most kinds of lasers go, is both bulky and fragile.

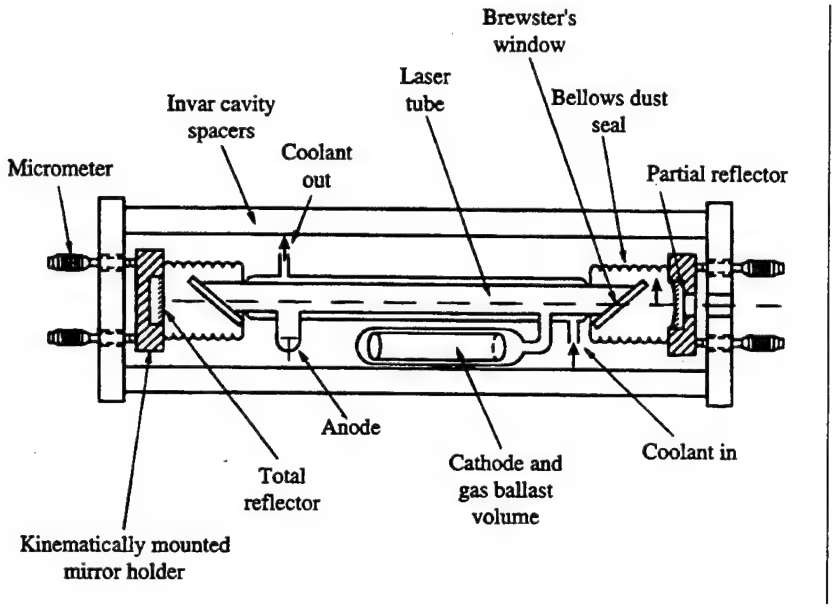

Figure 1-1. Typical Axial CO_2 Cavity Design (Davis, 1996)

An improvement on the glass tube design applicable at powers of 100 watts or less is to use a small cross section channel milled in a larger ceramic block. This reduces the fragility but only slightly reduces the size. In the 1980's two approaches to size reduction were investigated, shown in Figure 1-2. On the left is a multiply-folded intersecting waveguide lattice, also known as the Cantoni design, and on the right is a multiple U-fold resonator with prism U-folds, known as a Ferranti design.

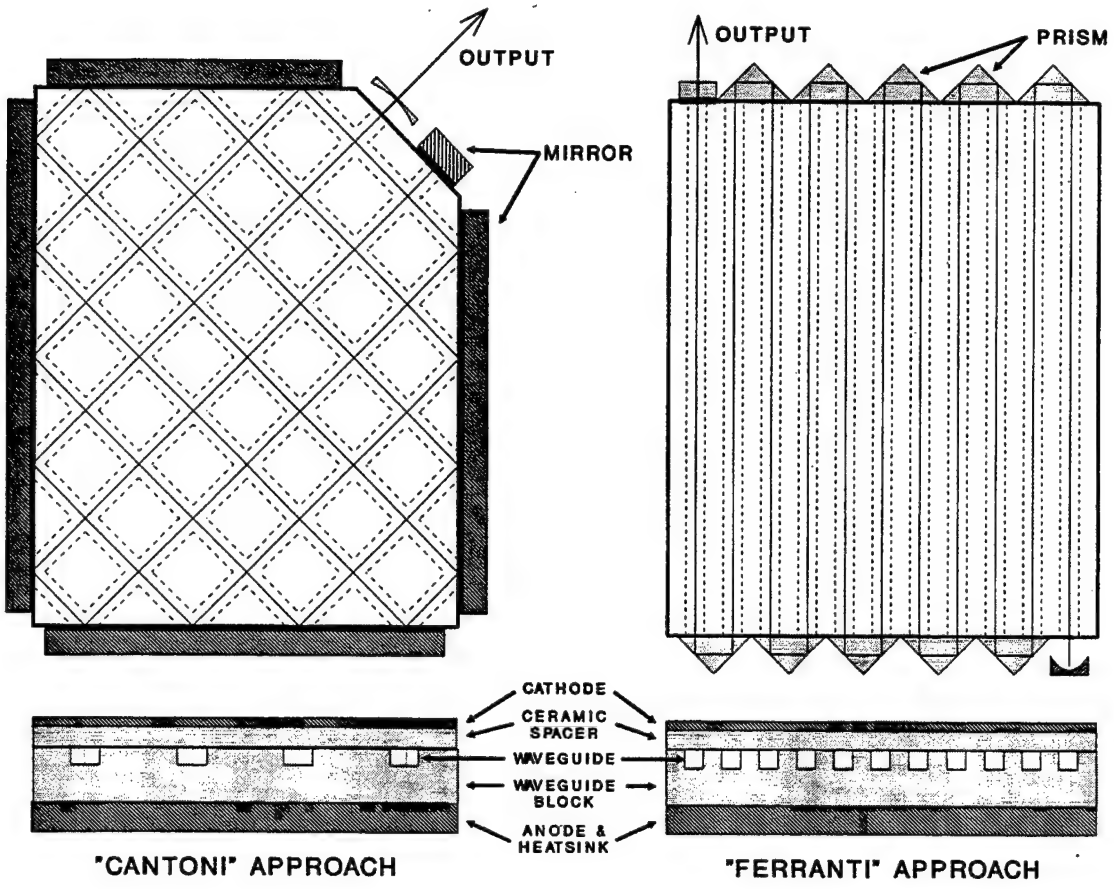

Figure 1-2. Left: Multiply-Folded Intersecting Waveguide Lattice (Cantoni) Design. Right: Multiple U-Fold (Ferranti) Design. (Courtesy Robert C. Harney)

Both configurations suffered from substantial loss at the bending points, and had limited power output due to the small ratio of gas to ceramic structure volume (<0.1).

Finally, a slab waveguide design (confinement of the optical beam in one orthogonal direction, unrestricted in the other two) has been used with an unstable resonator to produce on the order of a kilowatt of optical power from a

compact resonator. However, the beam quality and spectral content of the unstable resonator eliminated its use in many applications. (Further discussion of resonator design is included in Chapter II.) (Ross, 1989)

As an alternative, we consider the conceptual design shown in Figure 1-3 which attempts to preserve the slab waveguide but use a novel stable resonator. An original concept of Professor Robert C. Harney, Naval Postgraduate School, Monterey, California, this new design presents several immediate advantages at first glance. First, there is no glass necessary as a structural component. The cavity is essentially bound by the beam-handling mirrors and the slab waveguide. These are mountable in a simple box-like container which needs only to be vacuum tight to function properly. Second, the overall dimensions of the cavity give it a considerable size advantage; lateral dimensions are only a few inches, while vertical height is a fraction of that, owing to the tight waveguide gap of a few millimeters. Finally, the flat compact box shape lends an inherent mechanical ruggedness, portability, and stability to the system not found in many state-of-the-art models.

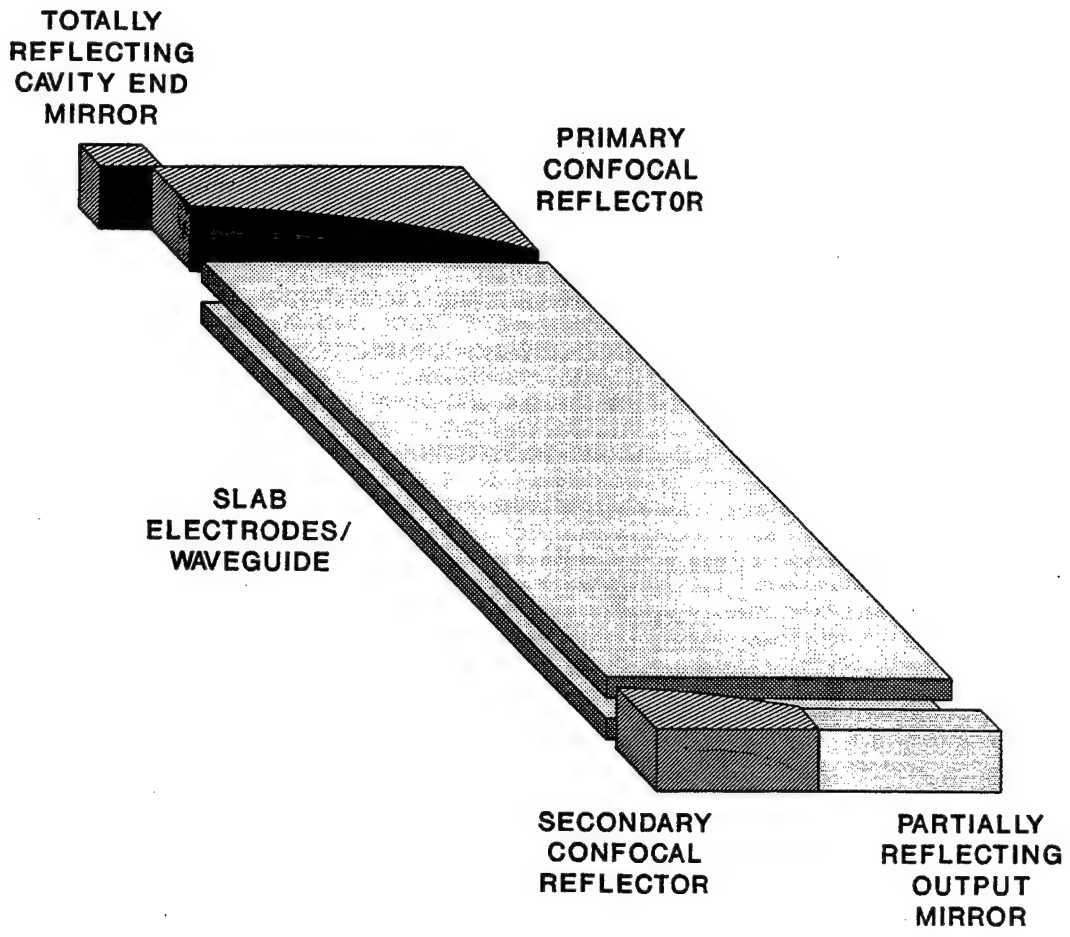

Figure 1-3. Prototype Laser Cavity Design
(Courtesy Robert C. Harney)

Most importantly, the system might offer a significant improvement in specific power (power per unit volume) over that which is associated with many current CO_2 laser systems.

B. BASIC SYSTEM CONCEPT

The gain medium is a 1:1:8 mixture of CO_2, N_2 and He. It is excited by a transverse radio-frequency (RF) field. The system is effectively sealed, and does not involve any flowing gas. For demonstration and testing purposes,

electrical excitation is provided by ordinary amateur radio equipment. The optics consist of three spherical cut-copper mirrors, and one zinc selenide (ZnSe) semi-transparent output coupler. Their function is to fold internally and to expand the beam within the optical cavity. Output of the laser is intended to be a monochromatic, collimated rectangular beam of infrared radiation with a nominal wavelength of 10.6μm. The maximum power output of the system is 50 watts, using the excitation equipment's available power and the industry average CO_2 efficiency of ten percent (10%). However, it is anticipated that the limited volume of the medium between the waveguide slabs may cap the maximum output at a lower level.

C. SCOPE OF ANALYSIS

This thesis research concentrated primarily on analyzing the optical cavity design. Using a commercially available optical design and analysis program, OPTICA©, the behavior of a collimated beam input was simulated as it passed through the resonator cavity. It was determined that the cavity, as designed, would not function as desired. Suggestions are included in this thesis, which,

if pursued, may alleviate or eliminate the problems that were found with in the original design.

Several of the laser's ancillary systems were examined as well with an eye to assembly of a low-cost breadboard concept demonstrator. The amateur radio equipment for the electrical excitation was researched and selected. Excitation circuit components were designed and quantified. Finally, a suitable vacuum chamber design concept was completed. All of these topics are discussed in subsequent chapters.

II. THEORY

A. CO_2 LASER THEORY

Prior to describing the proposed system in detail, it is helpful to review the fundamentals of carbon dioxide laser theory. The processes of excitation and emission, as well as the mechanisms of gain, amplification and oscillation that build upon these are central to a core understanding of any CO_2 laser's basic composition and workings. Using these as a foundation, comprehension and appreciation for the system design attributes and function will be more readily attained.

1. Molecular Excitation

Like any laser, CO_2 lasers produce optical energy on the principle of de-excitation of a medium from a prescribed upper energy level to a lower one, via stimulated emission. Unlike many solid state lasers, however, the CO_2 involves excitation and relaxation of molecular rotation-vibration states, rather than the energy states associated with orbiting electrons. The processes of creating and sustaining a discharge in the gas, pumping and de-exciting the gas molecules in the medium, and the various energy level transitions are a good starting point in gaining an overall understanding of the system.

a. Gas Breakdown and Electrical Discharge

Every laser's primary purpose is to produce coherent optical radiation. The first part of doing this is the transfer of electrical power to the lasing medium, which in this case is the mixture of carbon dioxide (CO_2), nitrogen (N_2) and helium (He). See Figure 2-1. Typically, as in this configuration, electrodes are placed inside the gas mixture along the cavity's central axis. This forces the discharge to occur along the axis of the cavity, spanning the majority of the lasing medium. In other configurations, as in the design considered in this thesis research, the electrodes are placed transverse to the cavity's optical axis. For either case, a high voltage AC or DC signal is imposed on the electrodes and an electrical field is generated between them. The gases, which are normally neutral, ionize or "break down," releasing electrons and positively charged molecular ions.

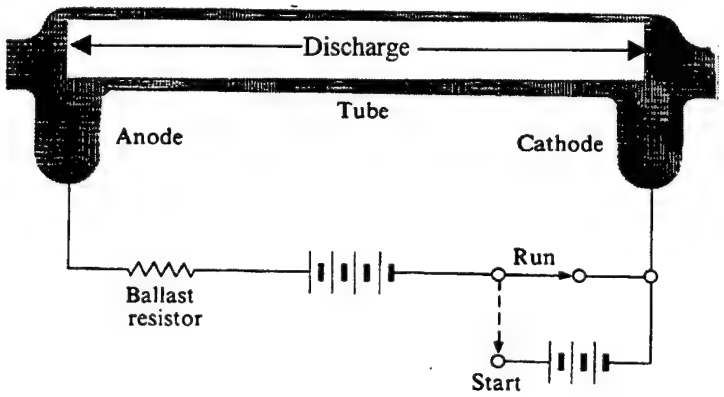

Figure 2-1. Typical Axial CO_2 Excitation (O'Shea, Callen and Rhodes, 1978)

Once free, the electrons are further accelerated by the imposed electrical field. The fast moving electrons collide with the heavier, slower gas molecules and excite them from their ground states up into higher rotational-vibrational (R-V) states. It is important to note that, unlike monatomic laser media (such as in the helium-neon laser) that rely upon radiative transitions between orbiting electron energy states, molecular gas lasers employ distinct R-V energy level transitions. The constituent atoms in each molecule can vibrate relative to each other and the molecule as a whole can rotate about its center of mass. Both types of motion are quantized, hence, molecules have many energy levels not found in single atoms, due to these extra mechanical degrees of freedom. (Siegman, 1971, 1986)

b. Fundamental Vibration Modes

Each distinct R-V state of molecular excitation is best described as an overall molecular rotation about the molecule's center of mass, combined with one of the three fundamental vibration modes, or their overtones. See Figure 2-2.

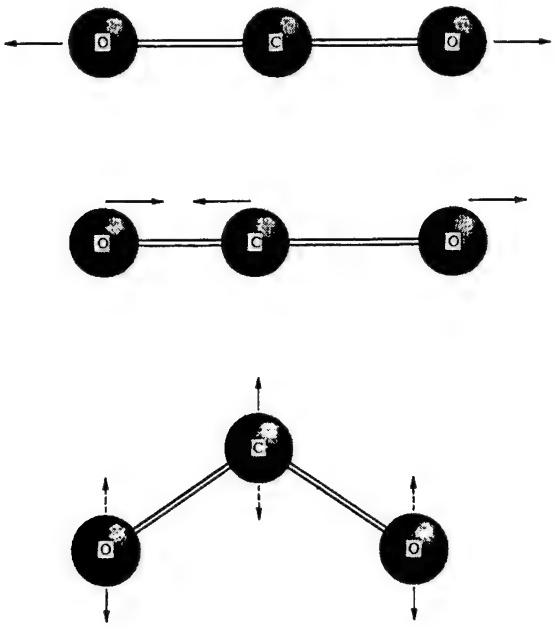

Figure 2-2. CO_2 Molecular Vibration Modes (Davis, 1996)

The mode seen in the center is the mode with the highest vibration frequency and is called the anti-symmetric stretch. In this characteristic motion the length of one C-0 bond increases as the other decreases: the molecule remains linear. In the vibration mode of next highest vibratory frequency, the symmetric stretch, (seen on top) the vibration is symmetric in the sense that the two oxygen atoms vibrate out of phase, while the carbon nucleus remains stationary. At bottom is the lowest fundamental vibration frequency mode, the bending vibration in which the molecule deviates from linearity. (Davis, 1996)

The respective natural frequencies (expressed as ν/c or wave numbers) for the fundamental modes are:

$f_1(\nu_1) = 1337\ cm^{-1}$ (symmetric stretch mode)

$f_2(\nu_2) = 667\ cm^{-1}$ (bending mode)

$f_3(\nu_3) = 2349\ cm^{-1}$ (asymmetric stretch mode).

(Siegman, 1971)

c. Molecular Energy Transitions

Because of the CO_2 molecule's quantized rotation, each vibration level is further split into much more closely spaced rotational levels, yielding literally hundreds of possible transitions up and down the energy level scale. This is illustrated in Figure 2-3. Emissive transitions shown are for a generic molecule dropping from a given energy level (v',J') to a lower one (v",J"). Here v signifies the vibration level quantum number, while J represents the rotational level quantum number. Downward transitions where J increases ($\Delta J = J'-J" = +1$) are called R-branch transitions and those where $\Delta J = -1$ are P-branch transitions. The number in parentheses in Figure 2-3 corresponds in each case to the lower rotational quantum number of the particular transition. In some molecules,

$\Delta J = 0$ transitions are permitted and are known as Q-branch transitions. Changes in J greater than one correspond to electric quadrapole and magnetic dipole transitions and are not relevant to CO_2 lasers. In CO_2 lasers, most transitions between vibrational energy levels are also limited to one, with $\Delta v = \pm 1$.

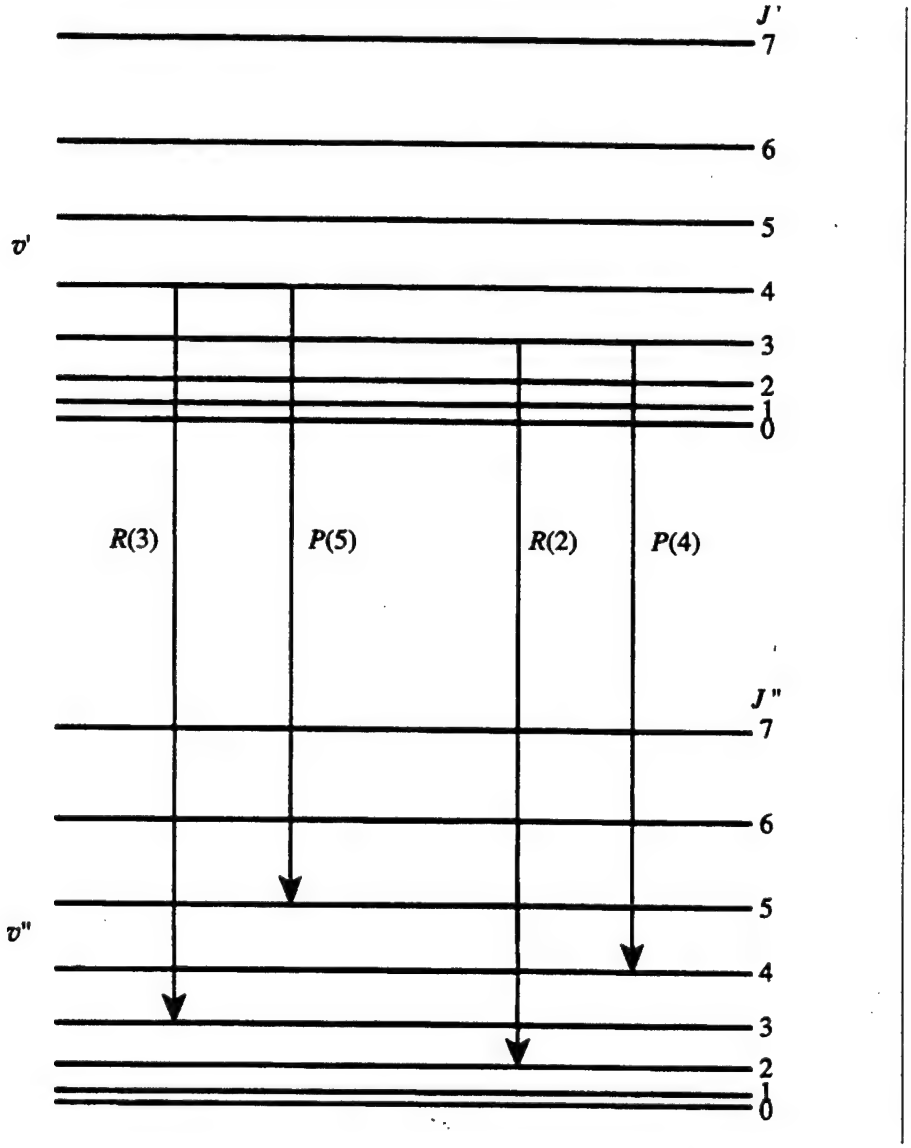

Figure 2-3. P-Branch and R-Branch Transitions.(Davis, 1996)

In summary, the relevant changes in R-V levels for purposes of this discussion are

$$\Delta v = \pm 1,$$
$$\Delta J = \pm 1, 0.$$

The difference in energy levels corresponds to the energy of the photon emitted during the downward transition, and therefore determines its wavelength by the equation:

$$\Delta E = \frac{hc}{\lambda} = h\nu .$$

ΔE is the change in molecular energy, h is Planck's constant ($h=6.63 \times 10^{-34}$ joule-sec), c is the speed of electromagnetic waves in a vacuum (3.0×10^{8} meters/sec), and λ and ν are respectively the wavelength (meters) and frequency (hertz) of the emitted photon.

There are several relevant emissive transitions for the CO_2 laser, producing photons where wavelengths cluster closely around a nominal 10.6μm value. They are:

P(18) ⇒ 10.57105μm,
P(20) ⇒ 10.59104μm,
P(22) ⇒ 10.61139μm,
P(20) ⇒ 10.63210μm.

The strongest of these is the P(20) line. An energy balanced equation for this transition is:

$CO_2(00^01)(J'=19) \Rightarrow CO_2(10^00)(J''=20) + h\nu\ (\lambda=10.59104\mu)$

Here, and elsewhere the notation $(n_1n_2^{\ell}n_3)$ contained in the set of parentheses immediately following the CO_2 symbol represents the energy quanta of each fundamental mode as previously discussed. The "ℓ" superscript represents the quantum number of degeneracy in the bending mode, due to the ability to vibrate in two orthogonal planes. Now with an understanding of CO_2 excitation on the molecular level, the concepts of absorption and emission, occurring in large collections of molecules, can be explored. (Davis, 1996)

2. Absorption and Emission

It is helpful to remember that the word "LASER" is actually an acronym standing for Light Amplification of Stimulated Emission of Radiation. The key ingredient here is the term stimulated emission. Like the marching men on the left side of Figure 2-4, photons that come from stimulated emission are in phase, and form coherent light. In contrast, incoherent light, a product of spontaneous emission, is modeled by the crowd on the right of Figure 2-4. Here, photons are emitted in random phase and direction, and therefore cannot build constructively.

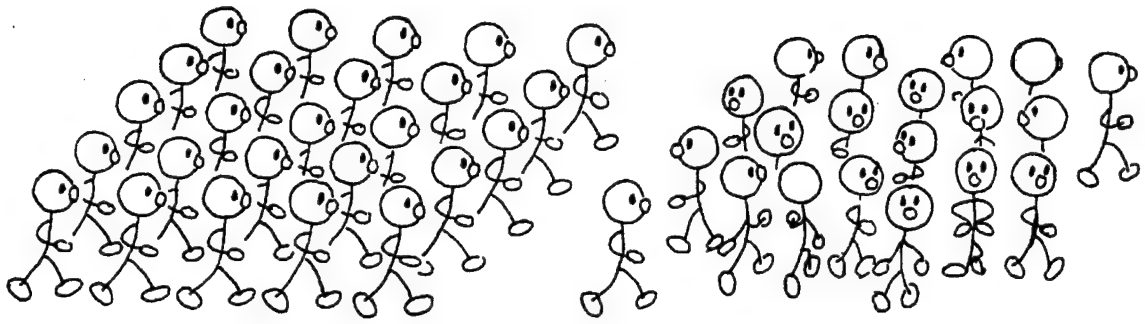

Figure 2-4. Left: Coherent Light. Right: Incoherent Light. (O'Shea, Callen, and Rhodes, 1978)

As the primary objective of the laser, the methods by which stimulated emission is achieved, to include those which deal with the processes, stimulated absorption and spontaneous emission, are worthy of some discussion. Stimulated absorption, or simply, absorption, is the process by which if a photon of energy $\Delta E = E_1 - E_o$ collides inelastically with a particle of the medium at ground energy level E_o, there will be a finite probability that the particle will jump subsequently to the excited state while the photon simultaneously disappears. This is illustrated in Figure 2-5(a). Spontaneous emission, shown in Figure 2-5(b) is a completely random event whereby a particle at E_1 suddenly de-excites to the ground state, releasing a photon of energy. Finally, in Figure 2-5(c), if a photon of energy $\Delta E = E_1 - E_o = h\nu$ encounters the medium already at E_1 there is a finite probability that the photon will cause

the medium to decay to the lower state and emit a second photon with the same direction, frequency and phase as the first one. The two photons go on to stimulate more emissions, and the process continues, producing coherent light.

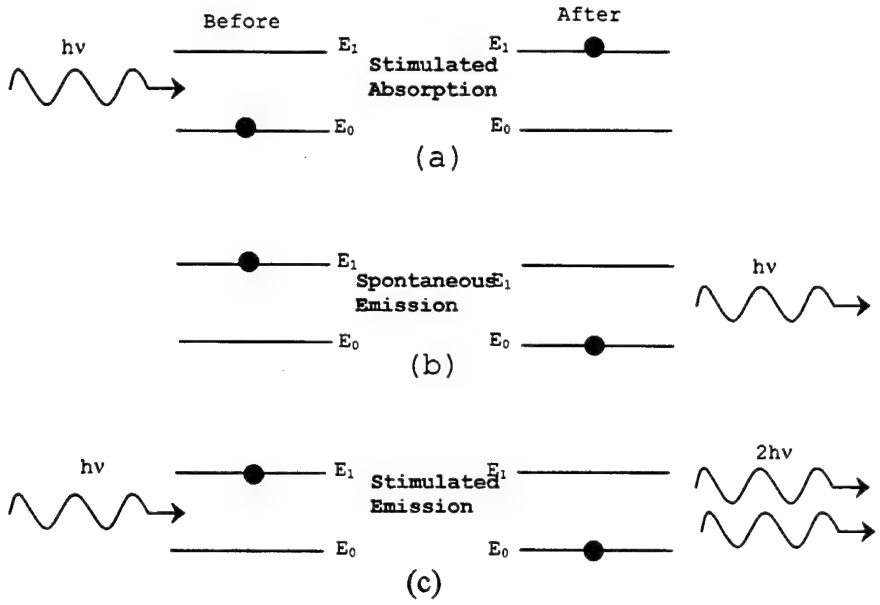

Figure 2-5. Emission and Absorption. (O'Shea, Callen, and Rhodes, 1978)

Thus, stimulated emission is what characterizes laser action.

It is helpful to review briefly the conditions under which stimulated emission occurs, as well as how it must successfully overcome absorption and spontaneous emission in order to produce gain. This involves a discussion of Einstein's coefficients, population inversion, and pumping,

the mechanism through which a population inversion is created.

a. Stimulated Absorption

Stimulated absorption is a necessary precursor in the chain of events leading to amplification. In the early part of this century, Einstein proved that for light incident on a given material, the rate of stimulated absorption was directly proportional to the population of atoms in the lower energy state (Day, 1997). In equation form this reads as:

$$\left(\frac{\partial N_n}{\partial t}\right)_{\substack{stimulated \\ absorption}} = -N_n \rho_\nu B_{nm}$$

where N_n is the population of atoms in the lower level E_n, B_{nm} is Einstein's coefficient for stimulated absorption from level E_n to level E_m, and ρ_ν is the spectral irradiance of the beam at frequency ν. In the special case that the radiation source is a blackbody,

$$\rho_\nu = \frac{8\pi h\nu^3}{c^3}\frac{1}{\exp[{}^{h\nu}/_{kT} - 1]}.$$

This means that the rate at which the population of particles in the lower energy level decreases is directly proportional to the population at any given moment. Thus, the more particles there are in the lower energy level, the

higher the probability is that a photon of the right energy $\Delta E = E_m - E_n$ will collide with such a particle and be absorbed. (O'Shea, Callen and Rhodes, 1978)

b. Spontaneous Emission

Like absorption, the rate of spontaneous emission is dependent on the upper level population. This does not conflict with the random nature of spontaneous emission; rather, it merely states that from a larger population at the upper level, one would expect a higher total number of spontaneous emissions over time. The rate equation for this is:

$$\left(\frac{\partial N_m}{\partial t}\right)_{\substack{spontaneous \\ emission}} = -A_{mn} N_m ,$$

where N_m is the population of atoms in the upper level and A_{mn} is the Einstein rate coefficient for spontaneous emission from level E_n to level E_m. (O'Shea, Callen and Rhodes, 1978)

c. Stimulated Emission

The rate equation for stimulated emission is very similar to that of absorption:

$$\left(\frac{\partial N_m}{\partial t}\right)_{\substack{stimulated \\ emission}} = -N_m \rho_\nu B_{mn} .$$

Again, the rate of stimulated emission varies with the population of the upper level.

Two important relations exist between the Einstein coefficients. The first is that under steady state conditions, the coefficients of stimulated absorption and stimulated emission are equal:

$$B_{mn} = B_{nm}.$$

The second ties the coefficient of stimulated emission to the coefficient of spontaneous emission:

$$A_{mn} = \frac{8\pi h \nu_{mn}^3}{c^3} B_{mn} \quad .$$

(Wilson and Hawkes, 1998)

While stimulated emission is the desired effect to support amplification, it is important to note that the major share of energy in the excited atoms is released through other mechanisms, most notably spontaneous emission and mechanical collisions. The reduction in beam irradiance at the frequency ν_{mn} is thus predominantly due to the absorption and subsequent spontaneous emission of wave energy. This does little in the way of achieving amplification, but the forced build-up of stimulated emission using a population inversion to sustain it will

overcome this loss, and lead eventually to the desired laser oscillation. (O'Shea, Callen, and Rhodes, 1978)

3. Population Inversion

a. Local Thermodynamic Equilibrium

Boltzmann's Principle is a fundamental law of thermodynamics which has a direct bearing on population inversion, the central prerequisite of a laser medium. It states that for a given collection of atoms or molecules in thermodynamic equilibrium, relative populations of the medium at energy levels E_1 and E_2 can be described:

$$\frac{N_2}{N_1} = e^{-\frac{E_2 - E_1}{kT}} .$$

With a simple algebraic manipulation, this leads to the relation:

$$\Delta N = N_2 - N_1 = N_1(1 - e^{-\frac{\Delta E}{kT}}) .$$

Thus, for a system in thermodynamic equilibrium, the lower level populations will always outnumber those of higher levels, as shown in Figure 2-6. Consequently, the total rate of stimulated transitions is biased in favor of absorption, which therefore dominates emission. In this way, the medium is overall attenuating. (Siegman, 1986)

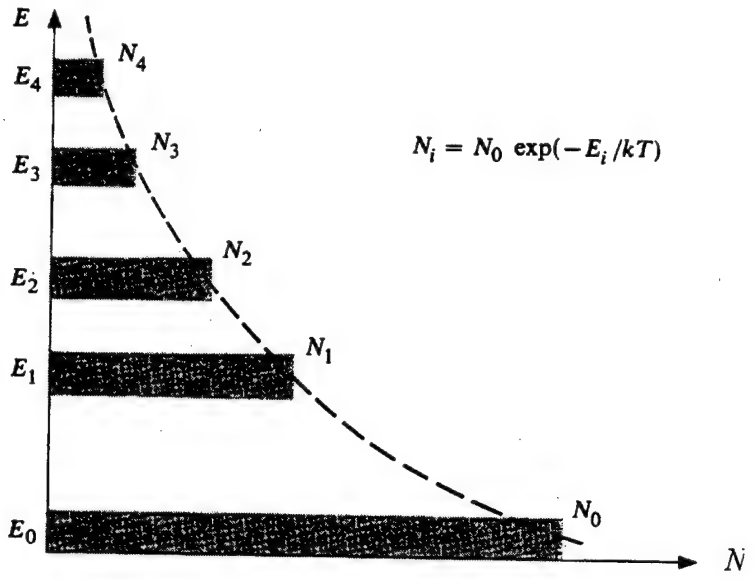

Figure 2-6. Boltzmann Distribution at Thermodynamic Equilibrium. (O'Shea, Callen, and Rhodes, 1978)

In order for the stimulated emission rate to surpass the absorption rate, there must be a way to stand the population difference on its head; that is, to create an upper level population that is greater than that produced in thermodynamic equilibrium. This situation is called a *population inversion*, and the mechanism by which it is attained is called *pumping*.

Figure 2-7 illustrates the relationship between pumping and population inversion in a generic four-level system. The population inversion is achieved by constantly exciting (pumping) the medium to some higher level E_3 from the ground state. From here the medium quickly decays to

the upper energy level E_2 and subsequently undergoes a downward transition to E_1 by stimulated emission. Because the ground state does not coincide with the lower laser level, a large population can exist in the ground state without the need for heavy pumping. The fast $E_1 \rightarrow E_o$ transition insures that few of the desired photons will be reabsorbed before exiting the medium. (O'Shea, Callen, and Rhodes, 1978)

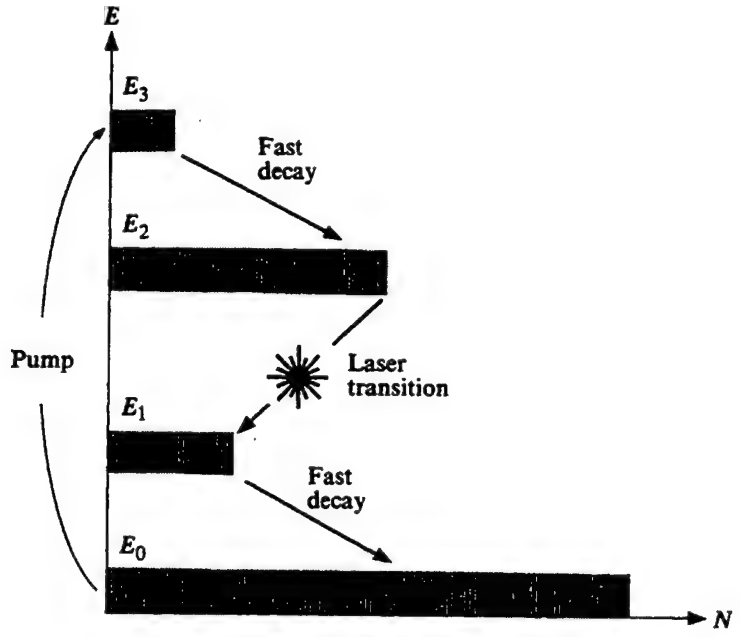

Figure 2-7. Four-level Laser System. (O'Shea, Callen, and Rhodes, 1978)

b. Roles of Nitrogen and Helium

Understanding that the CO_2 laser process depends first on the excitation of CO_2 gas molecules to the desired excited vibrational state (00^01), one can appreciate the

importance of doing so in the most efficient manner possible. It was found not long after the CO_2 laser's invention in the 1960's that the addition of nitrogen and later helium contributed greatly to the excitation efficiency. Nitrogen was discovered to be an excellent pumping medium, while helium provided a good means of de-excitation of the lower level to the ground state, thereby greatly increasing the laser efficiency.

In order to obtain a population inversion, there must be a mechanism known as pumping. This is the input of energy into the system such that, in spite of losses due to spontaneous emission, absorption, reflection, and scattering, relaxed atoms or molecules are continuously pushed back up to the upper lasing energy level. See Figure 2-8.

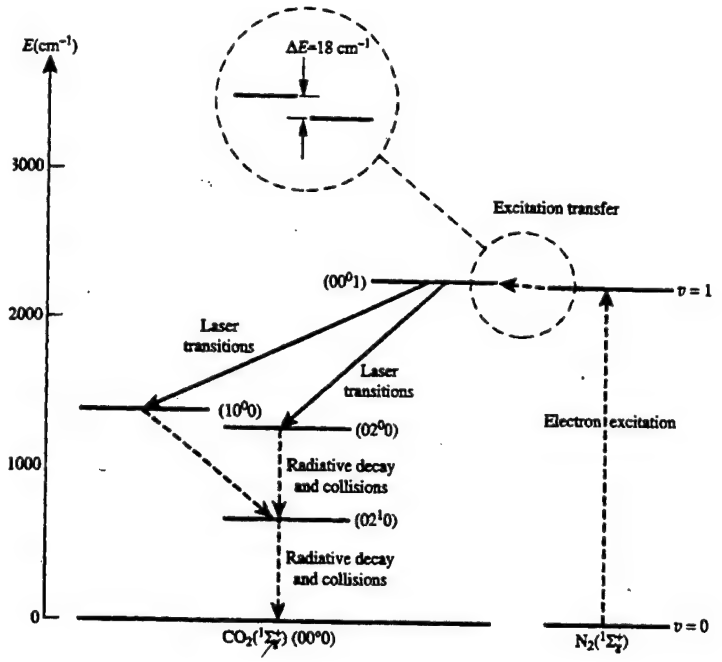

Figure 2-8. CO2, N2 Excitation Processes (Davis, 1996)

Nitrogen's contribution to pumping comes from the resonant transfer (through collision) of molecular vibration energy of excited N_2 molecules in their first excited state - $N_2(v=1)$ - to CO_2 molecules in the ground state $(00^0 0)$, thereby exciting the latter to the $(00^0 1)$ state. Since nitrogen has a zero permanent dipole moment, the nitrogen molecules electrically excited to $N_2(v=1)$ state cannot decay to the $N_2(v=0)$ state through electric dipole radiation. Because of this, the effective lifetimes of these states are governed by deactivation through collisions with other molecules, especially CO_2 (Patel, 1964).

The energy equation form of this appears as follows:

$$N_{2(v=1,\ E=2330.7\ cm\text{-}1)} + CO_2\ (00^00) \Rightarrow$$

$$N_{2(v=0)} + CO_2(00^01)_{(E=2349.7\ cm\text{-}1)} - 18.5\ cm^{-1}.$$

The quantitative contribution of nitrogen to the CO_2 laser cannot be understated. In one experiment, Patel reported a ten-fold increase in the laser's efficiency with the addition of nitrogen to carbon dioxide (Patel, 1965). While carbon dioxide lasers can operate in the absence of nitrogen, its value added as an efficient pumping medium far outweighs the marginal gain in simplicity of a one-gas laser design.

In a subsequent paper, he noted that the addition of helium to the gas mixture provided an additional eight-fold power output boost over that attained with the CO_2-N_2 mix (Patel, 1965). While early theories differed on the reason for this, recent analysis indicates that the helium primarily provides a collision based outlet of the lower laser level of carbon dioxide to its ground state, and also enables easier creation of a uniform gas discharge. These lower laser levels, the (10^00) and (20^00), are close enough in energy that they, too, constantly exchange energy through collisions. (Davis, 1996)

c. Beer's Law and Gain

The desired effect of stimulated emission in order to achieve amplification requires net gain, so that the stimulated emission process is not outweighed by the absorption process. While stimulated absorption describes the loss of incident photons on the molecular scale, Beer's law mathematically describes the overall macroscopic loss, or attenuation, of incident radiation as it travels through the lasing medium. Beer's law not only governs this large-scale process but stipulates the conditions required for gain, the artificially increased radiative beam intensity along the beam's direction of travel.

Beer's law is written in the general form:

$$I(z) = I(0)e^{-\alpha z}.$$

Here, I(0) is the irradiance of the beam at an arbitrary starting point, I(z) is the irradiance at some point at distance z along the optical axis from the starting point, and α_ν is the coefficient of absorption of radiation of frequency ν. If $\alpha_\nu > 0$, the relation basically states that given no external influences, the beam energy will be attenuated via the absorption and subsequent spontaneous emission of radiation as it traverses the chamber. But, if $\alpha_\nu > 0$, irradiance will increase as the beam propagates.

Straightforward manipulation of the rate equations and the Einstein coefficients shows that:

$$\alpha_\nu = \frac{-A_{mn}c^2 \nu g(\nu, \nu_{mn})}{8\pi \nu^3{}_{mn}}(N_m - \frac{g_m}{g_n}N_n) .$$

(Wilson and Hawkes, 1998)

A_{mn} is the coefficient of spontaneous emission, c is the speed of light, ν is the center frequency of beam's light, ν_{mn} is the transition frequency between energy levels, $g(\nu, \nu_{mn})$ is the line shape factor, N_m and N_n are the populations, respectively, of the upper and lower transition energy levels, and finally g_m and g_n are the levels' statistical degeneracy weights. The overall sign of α_ν is governed by the $N_m-(g_m/g_n)N_n$ term. It follows that for absorption or attenuation it must be negative. For the threshold of gain, whereby the exponent in Beer's law becomes positive and irradiance increases with length, the factor on the right must become positive, and the following must be true:

$$(N_m - \frac{g_m}{g_n}N_n) \geq 0 .$$

Rearranging terms, this leads to the condition:

$$\frac{N_m}{N_n} \geq \frac{g_m}{g_n}$$

for the onset of gain. This means that for amplification (gain) to occur, the population of atoms (or molecules, as with the CO_2 laser) in the upper excited level, E_m, must outweigh the population in the lower, relaxed state E_n. This again pertains to the population inversion requirement already discussed. (O'Shea, Callen, and Rhodes, 1978)

B. OPTICAL RESONATOR THEORY

A population inversion by itself does not make a laser. In order to function properly and produce useable optical energy, a device must produce enough stimulated emissions to overcome the combined loss effects of absorption, scattering, and miscellaneous loses. Because the amplification provided by most lasing media is only on the order of a fraction of a percent per centimeter, modern lasers - including the CO_2 - must be configured either to generate more power per unit length of optical axis or reduce the undesirable losses. Laser resonators, especially stable ones, actually accomplish both missions at the same time, using the feedback concept.

1. Feedback

A guitarist at a rock concert can get his instrument to groan, squeal, screech and produce many other unusual but mob-pleasing sounds by simply striking a note or chord

and then holding his guitar directly in front of the speaker. This allows the musical sound to feed directly back through the amplifier via the guitar's pick up located under the strings. The acoustic energy is subsequently re-amplified, fed back again through the amplification circuitry, and the process continues over and over until the desired cacophony is achieved. A similar effect is experienced with public address systems where the microphone is located too close to the output speakers (Day, 1997).

In both cases, the sound produced is the manifestation of positive feedback, a phenomenon common to many mechanical, electronic, optical, and acoustic systems where an oscillator's signal is repeatedly passed back through an amplifier in phase with itself, leading to increasing gain. A system so configured is called a positive feedback resonator, and in laser technology includes various optical and structural components. It is in this way the normally poor gain per centimeter of a single pass beam is greatly enhanced while the extensive loss mechanisms associated with the propagation of electromagnetic radiation are overcome to produce a steady state, highly coherent output. (O'Shea, Callen, and Rhodes, 1978)

Consider the stable resonator depicted in Figure 2-9 (a). Suppose that a medium with the appropriate population inversion is situated between the mirrors. Here, the beam of photons is reflected back and forth along the optical axis between the two mirrors many times. As it does so, the beam's photons trigger stimulated emissions producing still more photons which beget more stimulated emissions and so on, until the gain builds and a steady-state oscillation is created. Most of the beam's energy is confined to the region immediately around the optical axis; otherwise it would quickly "walk off" one of the end mirrors and fail to make a round trip through the resonator.

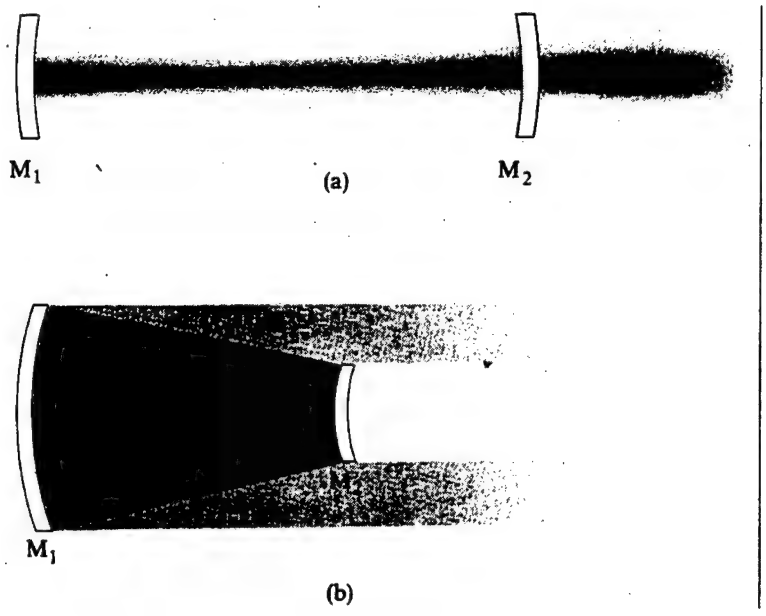

Figure 2-9. Basic Resonators: (a) Stable, and (b) Unstable (O'Shea, Callen, and Rhodes,1978)

Provided that the cavity length L is adjusted so that the net round trip phase change is a whole number of wavelengths, a highly collimated and coherent beam is produced.

The gain criterion for the onset of oscillation to occur after one round trip of the beam between the mirrors in this stable cavity is (O'Shea, Callen, and Rhodes, 1978):

$$G = R_1R_2\exp[2(\beta-\alpha_1)L] = 1.$$

Here, R_1 and R_2 are the mirror reflectivity constants, α_1 is the loss coefficient and L is the cavity length.
The threshold small-signal gain coefficient, β, is defined in the following equation (O'Shea, Callen, and Rhodes, 1978):

$$\beta = B_{nm}(N_m - N_m)\frac{h\nu_{nm}}{c}.$$

Again, B_{nm} is Einstein's stimulated emission coefficient, N_m and N_n are the populations of the upper and lower lasing energy levels (the difference between them being the relative population inversion), h is Planck's constant ($h= 6.626X10^{-34}$ joule-sec), and c is the speed of propagation of electromagnetic radiation in the medium.

Once more, note that the small signal gain depends on the magnitude of the population inversion. The small signal gain coefficient can be expressed in terms of the output and cavity losses in the following equation (O'Shea, Callen, and Rhodes, 1978):

$$\beta_{th} = \alpha_l + \frac{1}{2L}\ln(\frac{1}{R_1 R_2}) = \alpha_l + \alpha_o .$$

Here α_l refers to the cavity losses - absorption, scattering, and diffraction - and α_o is the loss owed to the laser's output. Thus, for steady-state oscillation, the gain by stimulated emission exactly balances the losses, including the intended output. (O'Shea, Callen, and Rhodes, 1978)

2. Stable Resonators

Again, the resonator shown in Figure 2-9(a) is considered to be stable. Geometrically, this means that after a finite number of beam bounces back and forth in the cavity, the wave front arrives back at its starting point with the same phase, wave vector, polarization and transverse amplitude distribution. Accordingly, any given beam segment must not diverge out of the cavity during the round trip. Constructive interference of the wave front ensues, allowing positive feedback and gain. With this and

any other stable configuration, the following equations apply as requirements for resonance:

$$L = \frac{n\lambda}{2},$$

$$\nu = n\frac{c}{2L},$$

where λ is the wavelength in the medium. This is to say that the total axial cavity length L must be equal to an integer number (n) of half wave lengths λ of the resonant frequency ν in order to satisfy the zero-amplitude cavity boundary conditions. Conversely, for a given cavity length the resonant frequencies allowed are described in the second equation. An equivalent condition that the beam return to its starting point in phase can be described by the following equation:

$$2kL = 2n\pi .$$

The factor k is the wave number in the medium. (Svelto, 1982)

To design a stable resonator, the following criteria for choosing the mirrors and cavity configuration apply:

$$0 < g_1 g_2 < 1, \text{ where}$$

$$g_1 = 1 - L/R_1,$$

$$g_2 = 1 - L/R_2 .$$

The factors L, R_1, and R_2 again are the cavity axial length, and cavity mirror reflectivities, respectively. (Svelto, 1982)

3. Unstable Resonators

Unstable resonators, while not as commonly employed in the laser industry, offer several advantages over their stable counterparts. First, unstable resonators make considerably better use of the available gain medium, as wide divergence of the beam quickly covers most of the available cavity volume, as seen in Figure 2-9(b). This may allow a higher system power-to-volume ratio, or specific power. Another advantage is high radiance emission; that is the power radiated per unit area of output per unit solid-angle. This is especially important because of the ability to create high specific intensity (or low divergence) beams with the use of suitable collimating optics. Finally, unstable resonators are particularly suited to high-gain, high efficiency media, as in the CO_2 laser. While the unstable resonator was not chosen as a prospective design in this project, its inherent advantages of high specific power and superior suitability for high gain media were adopted as desired characteristics in the conceptual design of an internally

folded stable resonator. The desire for a collimated beam output with no externally added optics necessitated the creation of a stable resonator design. (Dyer, 1992)

Because unstable resonator theory is not otherwise incorporated into the design concept presented here, it will not be discussed in detail. For a thorough treatment of unstable resonators and their applications, the reader is referred to P. E. Dyer's paper, "Unstable Resonators", from *The Physics and Technology of Laser Resonators,* Institute of Physics Publishing, 1989.

III. SYSTEM DESIGN OVERVIEW

Now with a basic understanding of laser operation in hand, and the generic CO_2 lasers in particular, the system level structure of the proposed Harney design for a compact CO_2 laser system finally can be examined. The design involves three subsystems: the electronics for excitation of the gas medium; the optical resonator; and the vacuum chamber containing the gas, wave guide and optical resonator. As shown in Figure 3-1, an RF signal generator is hooked to the parallel plate wave guide inside the vacuum chamber via a power amplifier, an antenna tuner, and cables.

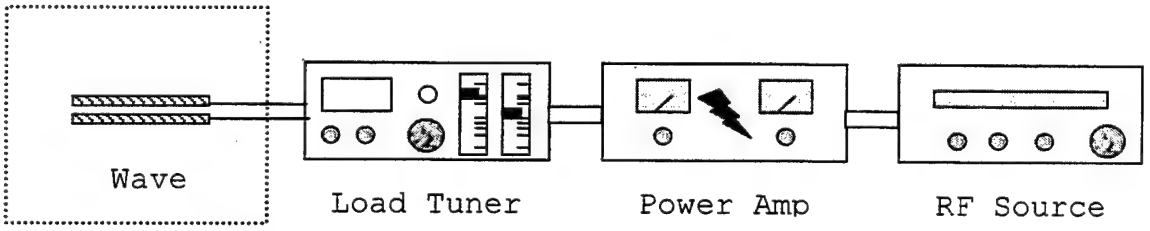

Figure 3-1. RF Excitation Schematic

The amplified RF signal produces a transverse oscillating electromagnetic field between the parallel plates of the wave guide. Ideally, this generates a uniform AC discharge in the volume of gas medium between

the plates. As a population inversion begins to develop and stabilize, and stimulated emission builds, it was hypothesized that a CO_2 laser beam should form on the folded

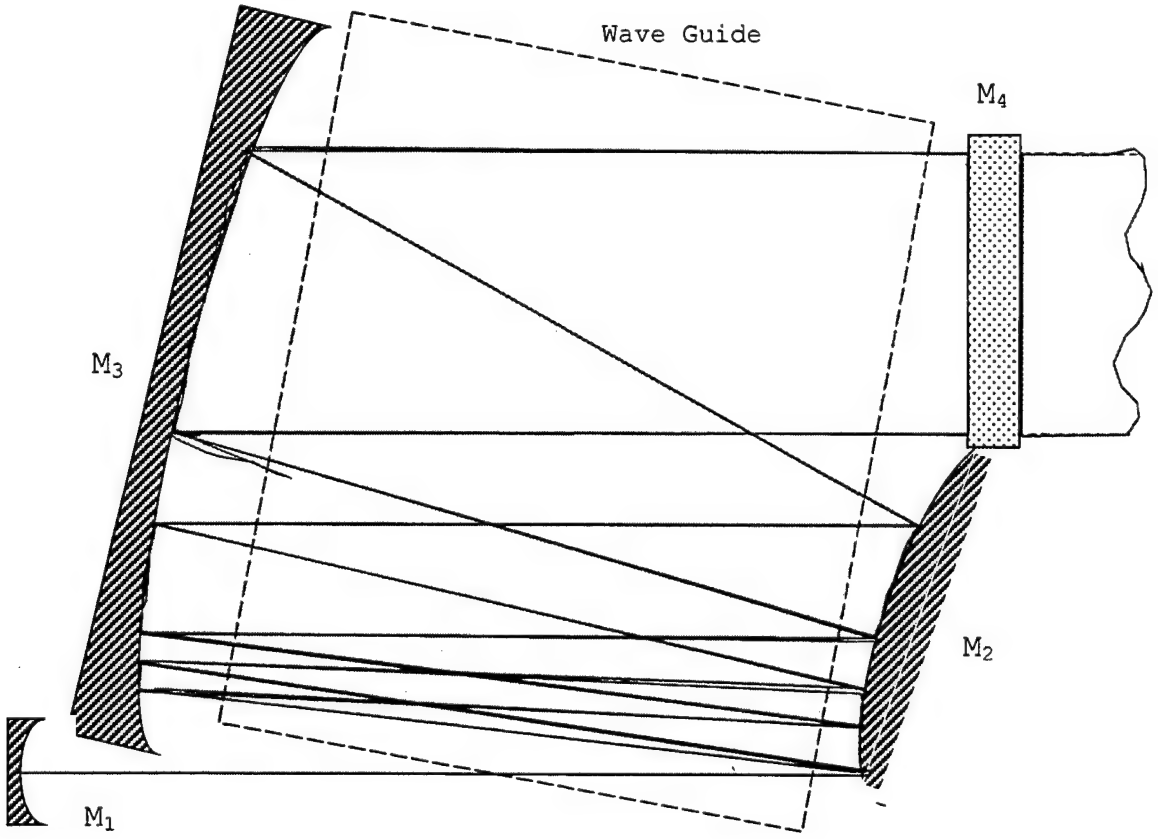

Figure 3-2. Resonator Top View

optical axis between the total reflector, M_1, and the secondary folding mirror, M_2, as illustrated in Figure 3-2.

As the beam bounces back and forth between the folding mirrors, M_2 and M_3, it also expands, using an increasing volume of the amplifying medium, and theoretically helping to boost the output power. Eventually the beam hits the

partially reflective output coupler mirror, M_4. At this point part of the beam energy is reflected back into the resonator while the remaining energy is transmitted as output. The relative amounts of transmitted and reflected energy are determined by the reflectance built into the output coupler mirror. With too small a reflectance, too much power escapes the system, resulting in low gain, in accordance with the previous discussion. Providing too high a reflectance can result in early gain saturation and undesirably low output power.

Ideally for optimum stable resonance, the beam is reflected back and forth in such a way that it eventually returns to an arbitrary starting point with the same phase and amplitude. Designing an optical configuration that achieves this is the major key to the successful employment of the system concept presented here. A detailed description of the optics is reserved for the next chapter, where the configuration above is presented again and optically analyzed.

A. RF EXCITATION

The use of radio frequency (RF) excitation presents several advantages over direct current (DC) excitation methods for the CO_2 laser. First, transverse RF requires

the application of a significantly lower voltage across the wave guide electrodes compared with that normally associated with a direct current excitation scheme. This is due in large part to the reduced gap between the electrodes. Whereas DC powered discharges are nominally in the tens of thousands of volts, because the electrodes can be spaced on the order of a meter or so apart, RF discharges can be sustained as low as the hundreds of volts. The lower voltage demand also goes hand-in-hand with an inherently compact optical design, allowing high specific power.

Second, RF excitation presents an advantage stemming from the positive impedance character of the discharge. Direct current discharges, in contrast, exhibit a distinctly negative differential impedance which is intrinsically unstable; as more DC power is sent through the gas, the impedance becomes less, causing still more power to be admitted and higher current to flow.

Third, because the electromagnetic field in a DC excited system is unidirectional, chemical interaction with the gas results in degradation of the cathode. This is virtually eliminated with an RF system due to its oscillatory nature. Taking this a step further, in

transverse excitation schemes, it is theoretically possible to eliminate the need for metal wave guides altogether because the RF power is capacitively coupled into the discharge. Some systems use a porcelain wave guide substrate, while others use a hybrid combinations of metal and porcelain, or other dielectric plates. (Dyer, 1992)

Finally, the equipment to set up RF excitation is readily available on the open market. This is not to say that the power supply and other items needed for ordinary high voltage DC excitation are uncommon or expensive, but it is clear that RF does not present a disadvantage due to a need for exotic components. An internet search for amateur radio equipment produced a multitude of available options. (Excitation in the 10-30 MHz region was chosen to permit the use of amateur radio electronics. Amateur radio, because of its large following, has the lowest dollar-per-watt cost of any frequency band.) A careful comparison of cost, effectiveness, and rapid availability led to the selection of the ICOM 735 HF transceiver as the RF source, the Ameritron AL-80B HF power amplifier, and the Ameritron ATR-15 load (antenna) tuner. (Note: there is little that is unique about these choices; their selection for this project does not imply an endorsement to the

exclusion of other candidate equipment with similar performance capabilities.)

1. RF Source: ICOM-735 HF Transceiver

The RF excitation source nominally chosen for this project is the ICOM-735, pictured in Figure 3-3.

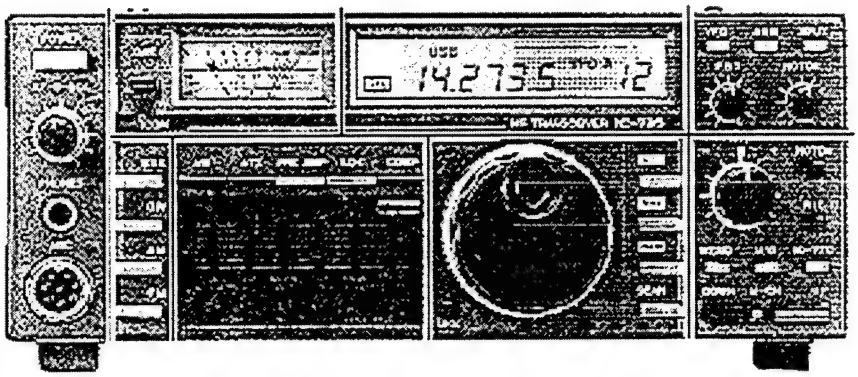

Figure 3-3. ICOM-735 HF Transceiver

It is an all band transceiver and general coverage receiver designed to operate throughout all high frequency (HF) amateur (HAM) radio frequency bands in the 10-160 meter wavelength range (1.8-29.7 MHz). It has the capability to function in single side band (SSB), continuous wave (CW), amplitude modulated (AM) and frequency modulated (FM) modes. It has the added capability of continuous tone transmission in the radio teletype (RTTY) mode with the use of an externally connected audio frequency shift keying (AFSK) device. This feature is desired one for excitation

of the laser gas, which demands continuous transmission of the RF power (100% duty cycle) through the wave guide to maintain the discharge. This mode should not be confused with continuous wave (CW) mode which actually involves a 50% transmission duty cycle. The output of the ICOM 735 transceiver is coupled via coaxial cable to the power amplifier, described below. Detailed specifications of the ICOM-735 are included in Appendix A.

2. RF Power Amplifier: Ameritron AL-80B

Considered to be the work horse of the system is the Ameritron AL-80B HF power amplifier, shown in Figure 3-4. Here, the output signal is taken from the ICOM-735 transceiver whose power gain is roughly 7 dB. (The

Figure 3-4. Ameritron AL-80B HF Power Amplifier

transceiver's maximum output of 100 watts fed to the AL-80B will produce approximately 500 watts of continuous power.) The unit uses a 50 ohm broadband Π-network tuned input to

maximize power throughput while minimizing reflected power back to the transceiver. At the output, a Π-Π-L network optimizes the Q-factor for further performance enhancement. Frequency band selection is made in similar fashion to that on the transceiver. The AL-80B's output is hooked to the ATR-15 antenna tuner, and subsequently to the load circuit, both of which are described next. A list of specifications of the AL-80B power amplifier is in Appendix B.

3. Load Circuit and Tuning Components

In order to meet the standing wave ratio requirements of the power amplifier, so as not to overheat it with reflected power and to couple power most efficiently to the wave guide, two important measures must be taken. First, the load circuit must be tuned as much as possible to accommodate the desired incoming RF frequency signal with a matched impedance. This involves estimating the impedance of the operating discharge, calculating the capacitance of the wave guide plates, and designing an appropriate inductor such that a combination of the three will reflect minimal, if any power, to the amplifier and match the output impedance of the amplifier to that of the load. Second, to minimize reflected power even further, a commercial RF antenna tuner can be installed between the

amplifier and the load. This will facilitate the best possible dynamic impedance matching and minimize or remove any reflected power not otherwise eliminated by the load circuit design itself.

a. External Load Tuner: Ameritron ATR-15

As a matter of practice, most amateur radio specialists include an antenna tuner in their rigs to facilitate the maximum transfer of power to their antenna load circuits. For this design, Ameritron's model ATR-15 antenna tuner, shown in Figure 3-5, was selected for its compatibility with their AL-80B power amplifier. When installed in the system, selection of the appropriate frequency band is made on the front panel controls. Total power throughput as well as standing wave ratios for both forward and reflected power levels are displayed, allowing continuous monitoring. The ATR-15 has a 1500-watt power handling capability, which for the sake of overload safety is sufficiently more than the amplifier's output. Other specifications of this unit are included in Appendix C.

Figure 3-5. Ameritron ATR-15 Antenna Tuner

b. Load Circuit

The load circuit associated with the wave guide is best modeled as a parallel combination of a resistor, a capacitor, and an inductor, as shown in Figure 3-6.

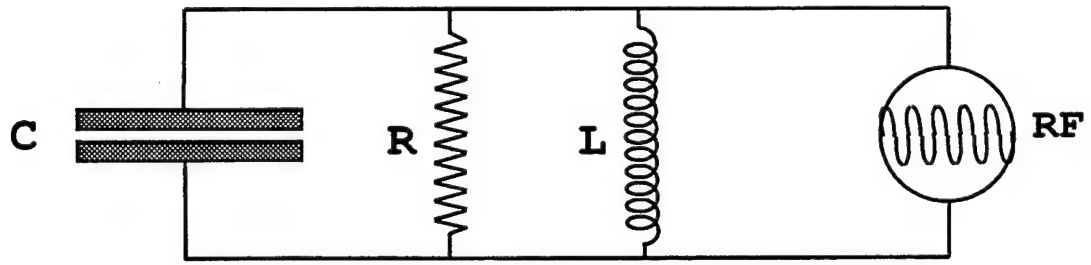

Figure 3-6. Equivalent Load Circuit

The resistor quantifies the impedance of the gas discharge, the capacitor represents the impedance of the parallel wave guide plates, and the inductor is added to facilitate a first order tuning of the load to the desired frequency, nominally taken to be 21 MHz. For the purpose

of simplifying this model, stray capacitance, inductance, and resistance quantities attributed to cables, chamber walls, optical supports, and other minor sources are considered negligible and are ignored.

The most uncertain quantity of the three parallel circuit elements is the resistance of the gas discharge. The complicated nature of any gas discharge impedance is such that it depends greatly on the temperature, pressure, and make-up of the gas mixture, as well as the wave guide dimensions and electrical characteristics of the applied power. It has been published, although not in a refereed forum, that the resistance can be approximated to first order using the following relation (Griffith, 1980):

$$R_g = \frac{m\nu d}{lwN_e e^2}.$$

Here, m and e are, respectively, the mass and charge of an electron, 9.1 x 10^{-31}kg and 1.6 x 10^{-19} coulombs; l and w are the lateral dimensions of the wave guide; ν is the collision frequency of electrons with the gas molecules, and N_e is the electron density. These latter two factors are calculated respectively from the following two formulae (Griffith, 1980):

$$\nu = \frac{eE}{2v_d m},$$

$$N_e = \frac{Pmvd}{V^2 Ae^2}.$$

Here, E is the strength of the electromagnetic field between the plates, V is the applied voltage, P is the power, and A is the cross sectional area of the wave guide perpendicular to the optical axis. The drift velocity, v_d, is empirically determined and itself depends on the gas mixture, pressure, wave guide dimensions and applied power. Using a 1:1:8 CO_2:N_2:He mixture at 20 torr pressure and 100 watts of RF power applied with a 1-kv voltage to a pair of parallel four-inch square wave guide plates separated by a 3 millimeter gap, the method outlined above predicts an approximate 300Ω discharge resistance. For the complete calculation, please see Appendix D. (Griffith, 1980)

Finding the capacitance of the parallel plate wave guide is comparatively simple. The following common formula is applied:

$$C = \varepsilon_o \frac{lw}{d}.$$

Here, the constant ε_o is the permittivity of vacuum, 8.85 x 10^{-12} farads per meter. Based on the same notional dimensions listed above, the wave guide capacitance is found to be 30 picofarads (30pf). (Halliday, Resnick, and Walker, 1993)

Finally, the inductance L required to rough tune the circuit is calculated using a well-known equation for the resonance frequency in a parallel RLC tank circuit of this kind:

$$2\pi f = 1/\sqrt{LC}\,.$$

Solving for L using C=30pF and a nominal frequency of f=21 MHz, L is found to be 2 microhenries (2 μH) (Simpson, 1987). A rugged inductor of this size can be constructed easily out of half-inch diameter plastic pipe wrapped with thirty turns of insulated heavy guage wire. See Appendix E for the complete design calculation.

B. GAS ENVIRONMENT CONSIDERATIONS

Properly enclosing the CO_2 laser system, including the mirrors and mounts, remote optical actuators, wave guide, RF feed cable, and the gas mixture, was a separate, iterative design process in its own right. Ideally, it should lead to the production of a very compact, modular, portable sealed system which accomplishes the central design objective of high specific power. Construction of such a system is certainly within the means of present technology. But, its final design should follow, not precede, the final optical configuration.

However, for the purpose of conducting functional testing of an analytically proven optics design, a simple, low cost chamber can be designed and constructed using readily available materials. Specific design blueprints are not presented here; instead, general design aspects of a basic cylindrical chamber are discussed which may save the reader considerable time and effort in producing an experimental prototype. The author's conception of such a system is included in Appendix F.

1. Chamber Dimensional Requirements

Because the system operates at a fraction of atmospheric pressure, the optical mirrors, the wave guide, and all supports and mounts must fit into a vacuum tight space in their optimal configuration (the latter is the subject of the next chapter). For the basic cylindrical chamber design shown in Appendix F, this means allowing a few inches over the maximum lateral spread of the optical cavity bench as configured in final form. Similar allowances should be made for vertical clearance from the tallest optical mount to the container top once the output coupler is aligned to the chamber output window. Careful measurements of the optical bench, along with reasonable

comfort regions will determine the necessary internal volume of the chamber.

2. Shell Material Selection

Three primary considerations for chamber material selection are strength, weight, and chemical properties. As built, the chamber should be able to withstand one atmosphere of external pressure for extended periods of time. The cylindrical shell design is most conducive to accomplishing this as well as minimizing the opportunities for vacuum leaks. Weight, as determined by material density, plays a significant role when one considers the relative ease by which a chamber can be maneuvered in the machine shop or laboratory. Steel densities run roughly three times the weight of most aluminum alloys, which are themselves considerably heavier than acrylics and plastics. Finally, outgassing can be a problem with organic materials like plastics, some of whose bonding agents tend to evaporate or deadsorb under vacuum. This not only weakens the material but also contributes unwanted gases to the lasing medium. Metals are not normally prone to this, and are stronger, but weigh considerably more.

As a suggested example of using off-the-shelf material, extruded Al-6061-T6 aluminum alloy tube, with an

inner diameter of fifteen inches, wall thickness 0.5 inch, and length of sixteen inches has a crushing pressure of nearly 10,000 p.s.i. (The complete calculation can be found in Appendix G.) Its weight is approximately 40 lbs., compared with nearly three times that for steel. (Baumeister, 1958)

3. Feed Through Fittings

In order to host the experimental laser, the chamber must accommodate the mechanical and electrical fittings necessary for air removal, gas infusion, powering the wave guide, and allowing the laser's output beam to pass out of the chamber. In addition, remote operators can be used to fine tune the positioning of the laser's optics while it is in operation. The vacuum, gas, pressure gauge, and RF feed cable fittings are standard hardware procurable on the open market. They may be installed anywhere on the sides, top or bottom of the chamber, as convenient, by simply milling the appropriate holes. The laser output window must be made of zinc selenide (ZnSe) or other infrared-transparent material, such as gallium arsenide (GaAs), and coated on both sides with an anti-reflective coating to enable maximum transmission of the output beam. Because of the brittleness of ZnSe, the window should be adequately thick

to withstand one atmosphere of differential pressure. A three-inch (3") window, masked to a two-inch aperture with an edge thickness of one-quarter inch (1/4") has been used reliably under similar vacuum conditions in the past (Wojtowich, 1988).

4. RF Confinement

Unchecked propagation of RF radiation from the electronics' side of the experiment is to be avoided at all reasonable cost. Several hazards apply here. First, high-intensity non-ionizing electromagnetic radiation presents a certain amount of danger to the health of unprotected personnel. Second, radio frequency interference (RFI) can adversely affect electronic systems in surrounding areas, and produce noise in the power distribution network of the surrounding building. Third, and not surprisingly, the frequencies used by the suggested excitation gear are intended primarily for use by amateur radio operators who are licensed by the Federal Communications Commission. The minimum consequence of a continuous, unchecked broadcast at any of these frequencies would be interference within a licensed radio band considered to be an emergency source of public communications. It also could lead to federal prosecution. It is therefore very important to take

reasonable steps to contain the RF radiation thoroughly. (American Radio Relay League, 1992)

One common technique used to contain RF in experiments such as these is the encasement of all potentially radiating components in a grounded metallic screen, wire mesh, or conducting box. The average size of the holes in the mesh or screen should be of a size considerably smaller than that of the RF wavelength. The mesh, screening, or box is then grounded to earth, and the RF energy is routed directly to this ground. Such a scheme is called a Faraday cage. By using a metallic conducting chamber (such as the aluminum alloy suggested previously) much of this Faraday cage is already in place, provided the chamber shell is grounded properly. Other parts of the chamber that are not conducting (for example,a transparent non-metallic top) can be covered or wrapped with copper mesh grounded to the metal shell. While RF cables leading to the chamber should be manufactured as shielded anyway, it is not a bad idea likewise to encase them in mesh covering or other effective shielding. One final alternative is to move the entire apparatus (including all electronics and optics) into a caged room or booth. This would allow less cumbersome of the chamber while providing adequate RF containment for the

purposes of avoiding an unintended broadcast. This would not necessarily shield personnel, however. For a detailed description of these and many other shielding techniques, the reader is referred to the American Radio Relay League's "Handbook for Radio Amateurs" listed in the references. (ARRL, 1992) Finally, after setting up the laser, and during its operation, a check for RF leakage using a suitable RF detector should be made.

IV. OPTICAL SYSTEM ANALYSIS

A. SPHERICAL CONCAVE-CONVEX CONFOCAL DESIGN

1. Description

As shown in Fig 3-2 (repeated here for convenience) the proposed optical system has four elements. Mirror M_1 is a 50mm-diameter concave reflector with a radius of curvature of ten (10) meters and focal length five meters (5m). The secondary reflector, M_2, is a 50 mm diameter spherical convex mirror with a 200 mm radius of curvature and a −100 mm focal length.

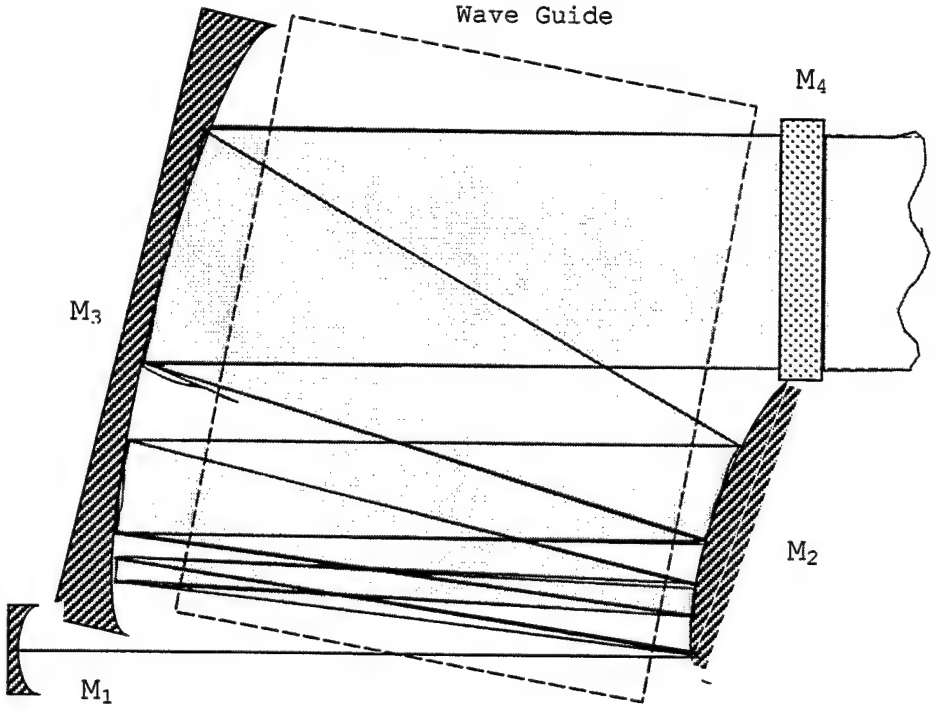

Figure 3-2. Optical Resonator Top View

The primary reflector, M_3, is a spherical concave mirror with radius of curvature 400mm and focal length 200mm. The primary and secondary reflectors are confocal, i.e., arranged in such a way that their focal points coincide. Finally, M_4 is the output coupler, a flat window with a 50% reflectivity coating applied to the wave guide side and anti-reflective coating on the other. While the output coupler is made of IR-transparent zinc selenide (ZnSe), the other three mirrors are all made of highly reflective (98%+) gold-plated copper substrate. The high reflectivity helps to maintain gain (see Chapter II), and the copper has a relatively low propensity for heat-related distortion given its high thermal conductivity (Beitz and Kuttner, 1994).

Conceptually, this cavity arrangement would achieve high specific power by folding the beam's length and expanding its cross section simultaneously, using the confocal mirrors. The folding would allow compression of the cavity's axial dimension requirement while magnification would expand the beam cross section, making better use of the available volume of gas medium between the wave guide plates. The magnification factor, equal to the ratio of the focal lengths of the primary and secondary

beam expansion mirrors, is equal to 2 in this case. (Higher magnification factors, while more enhancing of the beam size, would necessitate a larger spread of the mirrors to maintain a confocal arrangement.) The smaller concave reflector and output coupler would act to confine the beam at its ends as any pair of cavity mirrors in a standard axial plano-concave arrangement.

2. OPTICA© Simulated Optical Performance Results

The optical cavity design was analyzed for geometrical stability by Professor D. Scott Davis, using the commercial software program OPTICA©. The program is derived from, and operates with, another mathematical analysis package known as MATHEMATICA©. The OPTICA© program first takes as input the design characteristics of an optical system, including the dimensions of each component as well as those of the overall setup. It then employs a matrix-based ray tracing algorithm to determine the performance of the optical system based on the determined path of an arbitrary beam as it is reflected and refracted through the system's various lenses, mirrors and prisms. (A detailed explanation of matrix ray tracing analysis can be found in a number of references. An excellent one is in *Introduction to Optics*, by F. L. and L. S. Pedrotti, Prentice-Hall, 1987.)

A three-dimensional visual depiction of the system design is produced, along with the calculated trace of the beam's trajectory. The program provides the option of optimizing the initial design arrangement for maximum performance, by individual manipulation of the original design parameters. This feature was used to a considerable extent in the analysis. (A table of the input design values is included in Appendix H.)

The dimensions and characteristics of the optical components were entered in as data, along with those of the layout, i.e., spacing, tilt, axial displacement, etc. Figure 4-1 shows the resultant simulation.

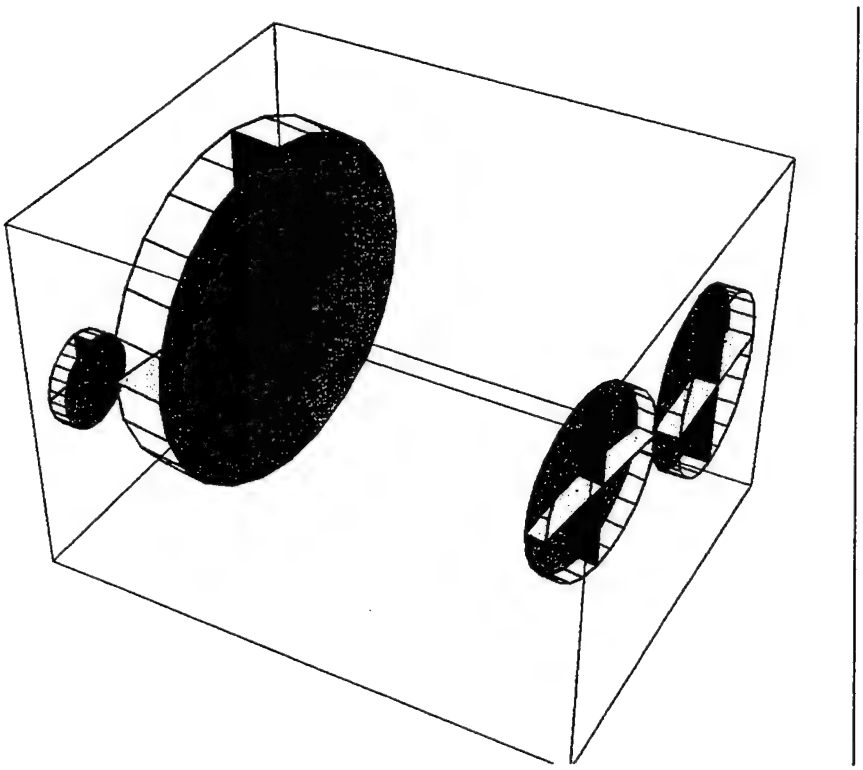

Figure 4-1. Original Design Configuration as Rendered by OPTICA©.

Next, a 2mm-diameter collimated beam originating at the center of M_1's position was created and the path of the beam generated. It should be pointed out that the beam itself is actually simulated with six separate parallel lines arranged in a hexagonal pattern, shown below as a cross section in Figure 4-2.

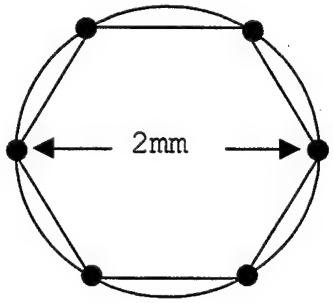

Figure 4-2. OPTICA© Hexagonal Simulated Beam Pattern

Thus, the circle encompassing this hexagon represents the beam, and has a diameter of 2mm. In this way, a better picture can be seen of how the beam is distorted by noting the changing positions of the six beam points relative to one another. The small concave reflector M_1 was removed during this trial in order to examine the behavior of the beam during one round trip through the cavity. The analysis results are shown in Figures 4-3(a) and (b).

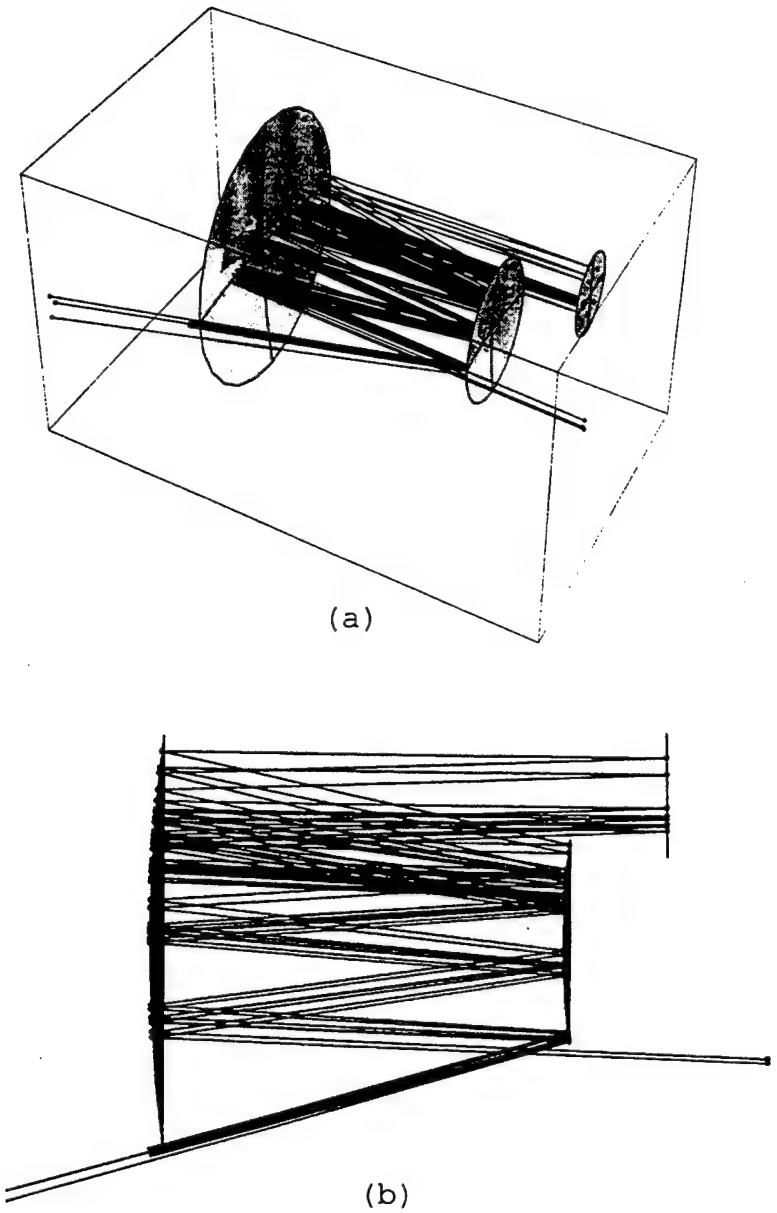

Figure 4-3. OPTICA© Trace of Collimated Beam Input.

Once it enters the confocal cavity, the beam initially behaves somewhat as desired. The six beam point trace lines expand as they are reflected back and forth. When they strike the output coupler, however, they are obviously

in a spatial arrangement that betrays significant deformation of the beam. In particular, the rays are no longer well-collimated because of spherical aberration. Then, as the beam is reflected back through the cavity, the deformation is only compounded. This is evidenced by the increasing uneven scatter of beam landing points along the mirrors, the inconsistent beam line bundle size, and the divergence of two beam lines out of the cavity at the lower right.

There are several possible sources of this condition. The most likely of these include spherical aberration, coma, and astigmatism. These are, respectively, the first and most influential three of the famous Seidel aberrations, which are aptly defined in numerous optical references, including *Optics* by Hecht, Addison Wesley Longman, Inc., 1998 (see List of References). In brief, spherical aberration, a problem indigenous to spherical mirrors, is attributed to the shifting of the focal point toward the mirror vertex with the departure of light rays from the paraxial region, as illustrated in Figure 4-4. Coma, another problem manifested with a departure from the paraxial region, is a variation in the transverse magnification of images as a function of the distance of

obliquely incident rays from the optical axis. An example of this is shown in Figure 4-5. Note that the spread of the rays increases with the off-axis angle. Finally, astigmatism is a difference in focusing point along the optical axis between rays that originate in the tangential and sagittal planes, as illustrated by the lens depicted in Figure 4-6. Here, lines S and T represent the different focusing point locations.

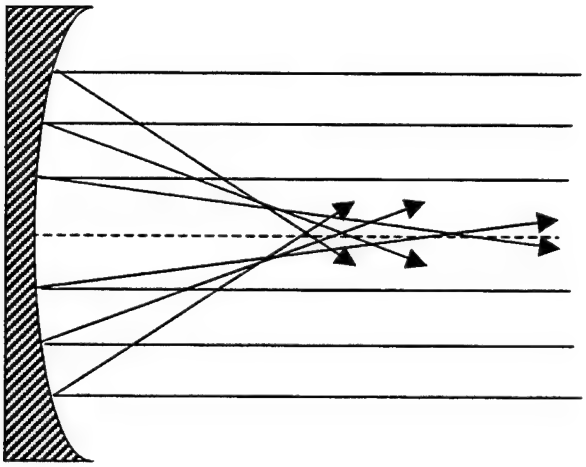

Figure 4-4. Spherical Aberration

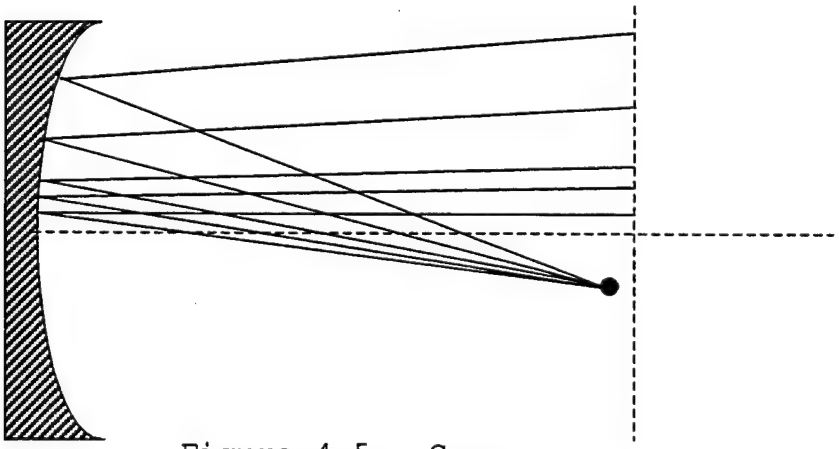

Figure 4-5. Coma

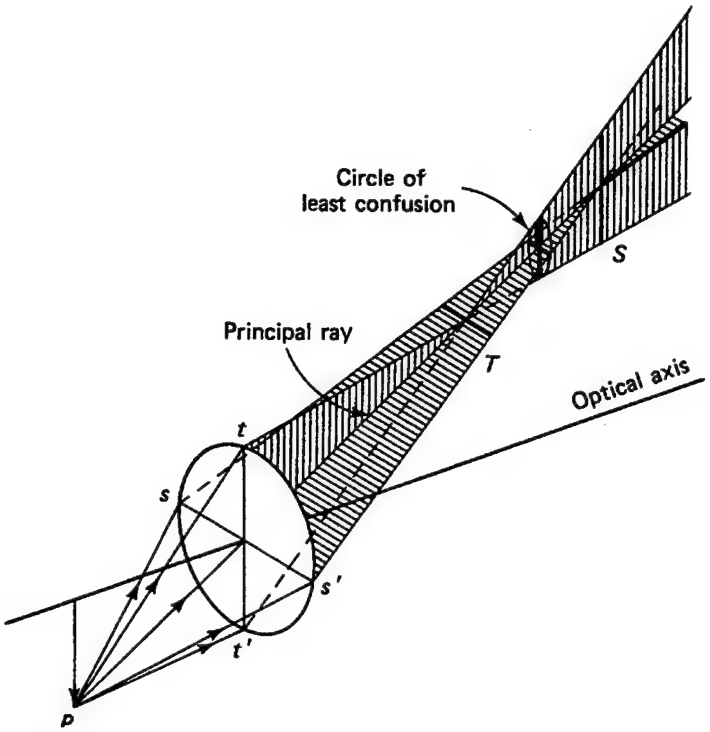

Figure 4-6. Astigmatism (Pedrotti and Pedrotti, 1987)

Because astigmatism is the least prominent of the three aberrations, its effects compared to the other two are already small. However, because the OPTICA© simulation that was run used an unobscured aperture with the non-paraxial resonator, the waveguide's restriction of beam propagation in the vertical direction was not simulated. Therefore, astigmatism's effect in an actual resonator prototype might be somewhat less.

In any case, the system as configured will not likely work well as a laser resonator because of the inability of the beam to be successfully returned back on itself in a closed-loop with an undistorted pattern. There are,

however, several possible remedies that may correct the distorting nature of the cavity design.

3. Suggested Modification: Schmidt Corrector Plate

One possibility is the modification of the output coupler to include a figure akin to that used in the Schmidt optical system, shown in Figure 4-7.

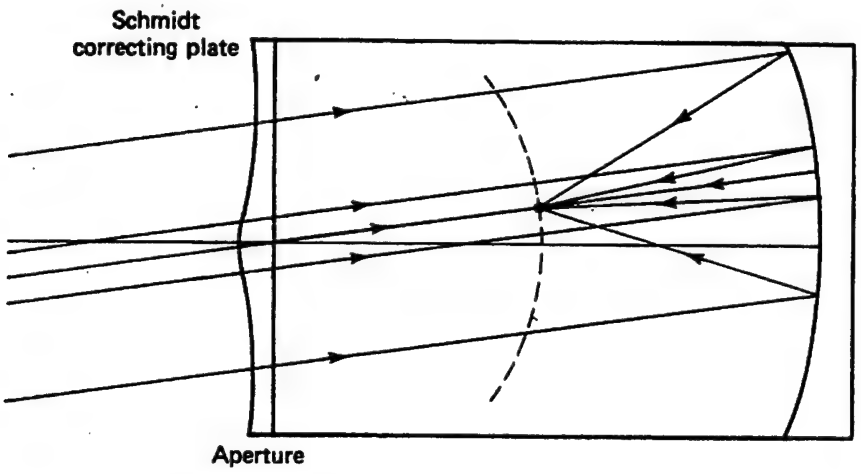

Figure 4-7. Schmidt Optical System. (Pedrotti and Pedrotti, 1987)

The corrector plate serves to distort incoming parallel ray bundles in such a way that, upon their reflection from the primary concave reflector at right, the loci of all focal points of the entering ray bundles would correspond to the dotted spherical surface in the middle. The resulting system is highly corrected for spherical aberration, coma and astigmatism. Similarly, if the output coupler of the laser cavity were to be cut as a suitable Schmidt corrector

plate, the focal points of beam reflections ideally would correspond to the surface of the spherical convex mirror. Obvious disadvantages of this scheme would include the complicated nature of designing and configuring the output coupler as a Schmidt plate, and the possible need to reconfigure M_1, the total reflector, as another Schmidt corrector plate. (Pedrotti and Pedrotti, 1987)

4. Suggested Modification: Aspherical Components

Another possible solution is to shift to using aspherical components in the confocal beam expander, e.g., a paraboloidal concave reflector and a hyperboloidal convex reflector. Since the proposed laser arrangement is functionally off-axis, this might also call for off-axis optics specially configured for this application (Hecht, 1998). The modified arrangement would resemble one half of the classic Cassegrain telescope, shown in Figure 4-8.

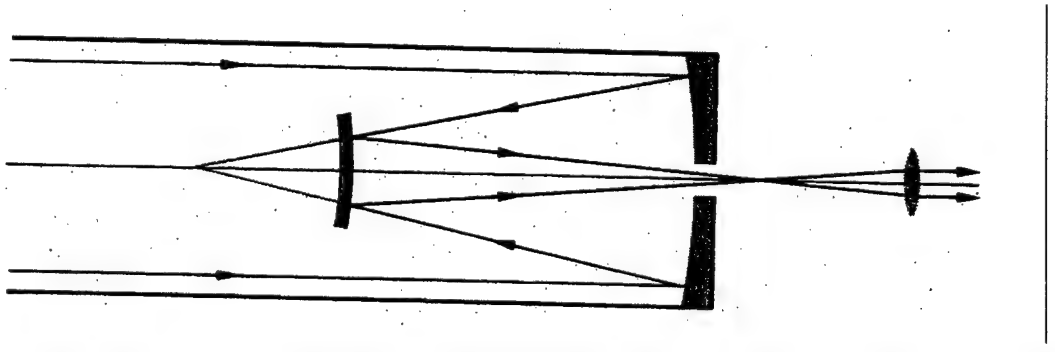

Figure 4-8. Classic Cassegrain Telescope. (Hecht, 1998)

It should be apparent that, aside from its spherical components, the proposed design already greatly resembles the Cassegrain arrangement. Within the context of some optical applications, such as reflector telescopes, considerable expense can sometimes be saved by substituting spherical optics for the more costly aspherical components. Use of aspherical hardware typically carries a higher price due to complicated manufacturing. In theory, such substitutions can be made wherever optical interaction is confined to the paraxial region; that is, where the distance of a light ray from the optical axis is relatively small in comparison to the radius of curvature of the component. This is illustrated in Figure 4-9 (Hecht, 1998) and by the following equation that quantifies axial deviation, Δx, as a power series function of y, the vertical displacement from the optical axis, and R, the radius of curvature:

$$\Delta x = \frac{y^4}{8R^3} + \frac{y^6}{16R^5} + \ldots .$$

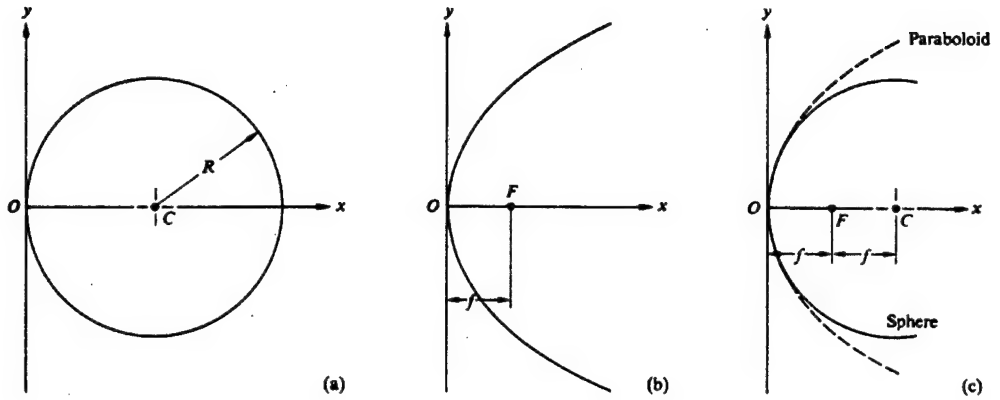

Figure 4-9. Comparison of Spherical and Paraboloidal Mirrors. (Hecht, 1998)

Thus, for a conceivable displacement of 100 mm, corresponding to the approximate upper edge of the primary reflector M_3, the theoretical axial deviation is approximately 0.2 mm in the first term, or 0.05 percent of the curvature. While an error of this size may not seem substantial for some optical applications, its diverging effects in a laser cavity would likely prove to be quite appreciable in practice. This is better understood when remembering the geometrical and quantitative requirements for resonance discussed in Chapter II. Given the gross amount of aberration apparent in the original cavity design, the use of uncorrected spherical components, while economical, would seem ineffective.

5. Waveguide Considerations

One final observation of the test results is the localized nature of the beam bundles, which may necessitate electrical modification of the waveguide. Concentrated beam bundles in certain areas, such as those in the lower part of the cavity will almost certainly have a tendency to draw increased electrical power from the discharge to these areas due to the higher localized conversion to optical power. This will lead to "hot spots" in the discharge, causing arcing in some places while starving the discharge in others. At best, this would result in inefficient, uneven power conversion. At worst, it could lead to severe plasma magnetohydrodynamic instabilities, effectively short-circuiting the large surface area of the waveguide. Therefore, once the optical cavity design has been perfected and the beam pattern is well known, the waveguide design may need to be modified geometrically or redesigned altogether to include a variable impedance distribution and to compensate for spatially variable power requirements.

V. CONCLUSIONS AND RECOMMENDATIONS

At first glance, the compact CO_2 laser design concept presents an innovative approach to the useful improvement of a proven technology. The miniaturization, structural edification, and specific power enhancement offered by the proposed laser more than justify the effort to explore its merits. The wide array of possible military and civilian applications of such a device speaks directly to the impetus of the concept's genesis. However, through the course of this analysis, several important conceptual flaws were discovered. If they can be ultimately overcome, construction of a working prototype can possibly be achieved.

The first and most prominent of these challenges is that a simple combination of spherical and plane mirrors will not work as a resonant cavity, due to the third order optical aberrations associated with such a configuration. Solutions might include the use of aspherical components, or replacing the output coupler and small concave mirror with Schmidt corrector plates, as discussed in Chapter IV. Other optical configuration changes may also be possible, but none are obvious at this point.

Second, the slab waveguide design may prove fallible if localized gain and oscillation lead to a power draw that overcome the guide's ability to sustain a uniform discharge. If this results in the serious degradation or cessation of oscillation, the slab waveguide will have to be rethought. One saving outcome may lie in the eventual optimization of the cavity design such that beam patterns no longer have this serious an effect. Alternatively, if the beam patterns become well known, construction of a distributed impedance waveguide may then be possible.

With all of this in mind, the following recommendations are made:

- Thoroughly reexamine the optical cavity design. In addition to those already presented, consider and possibly analyze other stable resonator designs.
- Consider the use of another resonator design, either a stable folded design like those mentioned in Chapter I, or an unstable resonator design, akin to that described in Chapter II. Any of these would seem well suited to the use of a slab waveguide. The folded configurations would be ideal for a high-quality beam application, and the unstable resonator would lend itself to simple,

large power needs due to the uniform, wide shape of the beam and a lesser likelihood of power hot spots.

- For each alternative design considered, conduct an intense, comprehensive simulation of the proposed arrangement. More than one simulation program may be helpful. This will provide a solid foundation for eventual construction of a working laser and a baseline of comparison for theoretical and experimental performance.

APPENDIX A. ICOM 735 HF TRANSCEIVER

1-1 GENERAL

Frequency Coverage: Ham Bands 10-160m (1.8-29.7 MHz)
Usable Temperature Range: -10°C ~ +60 °C (+14 °C ~ +140 °C)
Frequency control: CPU based 10Hz step digital PLL synthesizer. Independent Transmit/Receive frequency available.
Frequency readout: 6 digit 100 Hz illuminated LCD
Frequency stability: <±200Hz from 1 minute after switch onto 60 minutes.
Less than <±30Hz after 1 hour at 25 °C
Less than <±500Hz in the range 0~+50 °C
Power supply requirements:
13.8V DC±15%(negative ground)
Current drain 20A max @ 200W input
AC power supply is available for AC operation
Current drain (@13.8V DC)
Transmitting at 200W input: ~ 20A
Receiving:
At max audio output ~ 1.5A
Squelched ~ 1.2A
Antenna Impedance: 50Ω unbalanced
Weight: 5kg
Dimensions (mm): 94(H) x 241(W) x 239(D)

1-2 TRANSMITTER

RF Power: SSB: 200W PEP input
CW: 200W input
AM: 40W output
FM: 200W input
Continuously adjusable output power from 10 watts to maximum.
Harmonic output: >40dB below peak power output.
Spurious output: >50dB below peak power output.
Carrier suppression: >40dB below peak power output.
Unwanted sideband: >50dB down at 1000Hz AF input.

1-3 RECEIVER

Receive system: Triple conversion superheterodyne with push-to-talk switch and scanning buttons.

Receive modes:	A3J (J3E) SSB (Upper & Lower Sideband	
	A1 (A1A CW	
	A3 (A3E) AM	
	F3 (F3E) FM	
Intermediate frequencies:		
	1st: SSB, AM,FM	70.4515 MHz
	CW	70.4506MHz
	2nd: SSB, AM,FM	9.0115MHz
	CW	9.0106MHz
	3rd: SSB,CW,AM,FM	455kHz
Sensitivity:	SSB,CW	
(PRE AMP ON on 1.6~30MHz)	0.1 - 1.6MHz	<1.0μv for 10dB S/N
	1.6 - 30MHz	<0.15μv for 10dB S/N
	AM (When selecting NARROW FILTER)	
	0.1 - 1.6MHz	<6μv for 10dB S/N
	1.6 - 30MHz	<1μv for 10dB S/N
	FM	
	1.6 - 30MHz	<0.5μv; 12dB SINAD
Squelch sensitivity:	FM 0.3 μv	
Selectivity:	SSB,CW	2.3kHz/-6dB,4.0kHz/-60dB
	AM	6.0kHz/-6dB, 18kHz/-50dB
	FM	15kHz/-6dB, 30kHz/-60dB
Spurious and image Response rejection:	>80dB	
Notch filter attenuation:	>30dB	
Audio output:	>3W/10% distortion with 8Ω load	
Audio output impedance:	8Ω	

(ICOM Inc., 1990)

APPENDIX B. AMERITRON AL-80B AMPLIFIER

Input: Circuit type: Pi-network, slug tuned coils
Maximum VSWR at resonance: 1.3:1 or less
Minimum 2:1
VSWR bandwidth: 20% of center frequency
Maximum drive power permissable: 100 watts
Typical drive for full power output: 85 watts
Output: Typical SSB PEP voice operation: 1000 watts
Typical CW continuous operation: 800 watts1/2 hour
PEP two-tone test: 800 watts
1/2 hour continuous carrier (RTTY): 500 watts
Power Supply:
Circuit type: full wave voltage doubler
No load voltage: 3000 V
Full load voltage: 2700 V
Full load current: .450 amp
Regulation: 10%
Transformer: 26 lb.
Capacitors: 26 mFd total, computer grade
Maximum draw at rated output: 12 amps at 120 Vac 50/60 Hz
Tubes: Type: Eimac 3-500Z
Continuous dissipation: 500 watts
Warm-up time: 5 seconds

Metering:
Multimeter: HV, FWD Power, RF Power, SWR, ALC, ALC set.
Current Meter: plate and grid current

ALC: True ALC 0-10V negative, front panel adjust
Efficiency CW: approximately 66% or greater
Efficiency SSB (envelope crest): approx. 66% or greater
MARS/WARC: yes, set to nearest amateur band

Keying: Keys amplifier when grounded, +12Vdc open circuit and supplies,100 mA when grounded, built-in back-pulse canceling diode, protects the exciter.

RF Connectors: SO-239
Line Connector: NEMA5-15P, standard 120V

Dimensions: 15 1/2" D x 14 1/2" W x 8 1/2" H
Operating Weight: 48 lb.
Shipping Weight: Unit,54 lb., Tube, 3 lb.

Frequency Coverage:
Domestic model: 160, 80, 40, 30, 20, 17, 15 meters. 10/12 meters with modification.

(Ameritron Corporation, 1999)

APPENDIX C. AMERITRON ATR-15 TUNER

The Ameritron ATR-15 is specially designed for today's new breed of maximum legal limit amplifers. These "super power'' amplifiers can deliver 1500 watts of RF envelope power!

The ATR-15 easily handles full legal power on all modes and all HF amateur bands above 1.8 MHz (1kW for 1.8 MHz). It lets you crank up your power without fear!

It's made by the company with years of high power experience: Ameritron -- the high power specialist.

A heavy duty silver plated bandswitch with nine parallel wiper contacts -- each rated at 7 amps -- virtually eliminates switch failure.

Two transmitting variable capacitors -- each rated at 4.5 KV -- can pass amps of RF current effortlessly for trouble-free operation.

It covers 1.8-30 MHz continuously.

An illuminated peak reading SWR/ Wattmeter reads 2000 or 200 watts full scale. Meter lamp requires 12 volts.

Antenna switch lets you select 3 coax lines, random wire or balanced line. Direct position lets you select external dummy load or tuner bypass.

For balanced lines you get a husky two core Teflon wound current balun that's superior to the voltage baluns used in most antenna tuners.

Why is it superior? Because the current balun minimizes feedline radiation and reduces field pattern distortion, TVI and RFI.

The ATR-15 is fully shielded in a solid steel cabinet. It measures a perfect 5 1/4" H x 13 1/4" W x 13 1/2" D.

(Ameritron Corporation, 1999)

APPENDIX D. CALCULATION OF GAS DISCHARGE IMPEDANCE

Since the RF discharge impedance is inherently dynamic with the various parameters of the power circuit and the gas mixture properties, it is important to note that any impedance values determined using the formulae in this section are not assumed to be fixed or exact. Rather, they should serve to provide the experimentalist with an idea of the order of magnitude of impedance to expect under reasonable conditions.

Using the cited reference (Griffith, 1980) as a guide, a first order approximation of the nominal discharge impedance (considered a pure resistance) was made using the following formula:

$$R_g = \frac{m\nu d}{lwN_e e^2},$$

m= mass of an electron, 9.31×10^{-31} kg,

d= parallel plate gap, 3×10^{-3} m,

l= lateral length of the wave guide plates, 100mm (4 inches),

w= lateral width of the wave guide, 100mm (4 inches),

ν = collision frequency:

$$\nu = \frac{eE}{2v_d m} \quad \text{(m/sec)},$$

N_e= electron density:

$$N_e = \frac{Pmvd}{V^2 Ae^2} \quad (\mathrm{m}^{-3}) .$$

We begin with calculation of the electrical field:

$$E = \frac{V}{d} = \frac{1000v}{3x10^{-3}m} = 3.33x10^5 V/m .$$

The value of V=1000 volts is a typical rms output voltage for the chosen power amplifier within the range of 100-500w. From this and a particle density of N=6.42 x 10^{23} (calculated from the ideal gas law, at 20 torr and 300K) we get the ratio E/N = 5 x 10^{-15} v-cm^2.

Next, we determine the drift velocity by inputting this value of E/N into the graph below (Figure 6 of [Lowke, Phelps, and Irwin, 1973] and extrapolating to get an approximate value of v_d=3 x 10^5 m/sec.

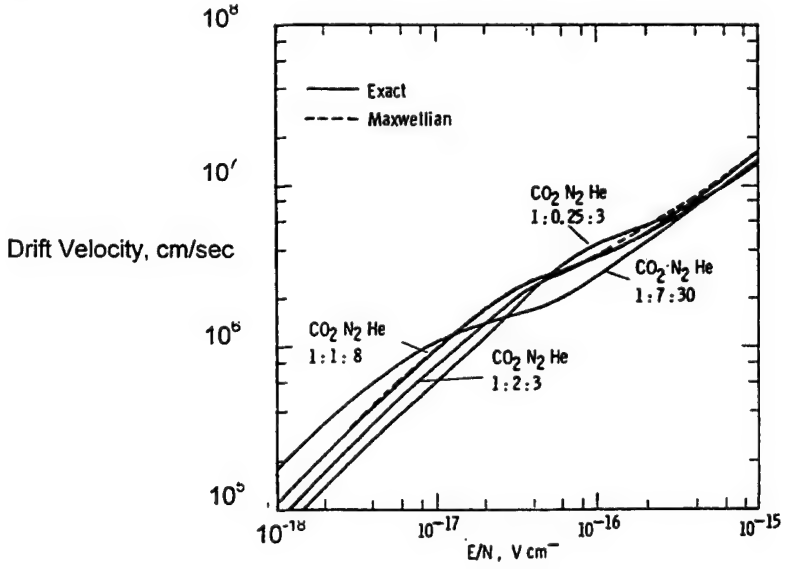

Inserting this and the value for E into the equation for collision frequency yields:

$$\nu = \frac{eE}{2v_d m} = \frac{(1.6x10^{-19} coul)(3.33x10^5 V/m)}{2(3x10^5 m/\sec)(9.31x10^{-31} kg)} \cong 10^{11}\sec^{-1},$$

and subsequently:

$$N_e = \frac{Pm\nu d}{V^2 Ae^2} = \frac{(100W)(9.31x10^{-31} kg)(10^{11}\sec^{-1})(3x10^{-3} m)}{(1000V)^2(3x10^{-3} m)(100x10^{-3} m)(1.6x10^{-19} coul)^2} \cong 4x10^{15} m^{-3}.$$

And, finally,

$$R_g = \frac{m\nu d}{lwN_e e^2} = \frac{(9.31x10^{-31} kg)(10^{11}\sec^{-1})(3x10^{-3} m)}{(100x10^{-3} m)(100x10^{-3} m)(4x10^{15} m^{-3})(1.6x10^{-19} coul)^2} \cong 300\Omega.$$

APPENDIX E. LOAD CIRCUIT TUNING INDUCTANCE

The following formula determines the inductance per unit length for a solenoid:

$$L/l = \mu_o n^2 A .$$

Here, l is the length of the solenoid, n is the number of turns per unit length, A is the cross sectional area, and μo is the permeability of free space, 1.26 x 10-6 henrys/meter. Rearranging this equation and solving for the length l:

$$l = \frac{L}{\mu_o n^2 A} .$$

Substituting in the tuning inductance L=2μH, and the appropriate values for a half-inch diameter hollow solenoid with ten (10) turns per inch of insulated wire, one finds a necessary length of three inches (3"). (Halliday, Resnick, and Walker, 1993)

APPENDIX F. VACUUM CHAMBER CONCEPTUAL DESIGN

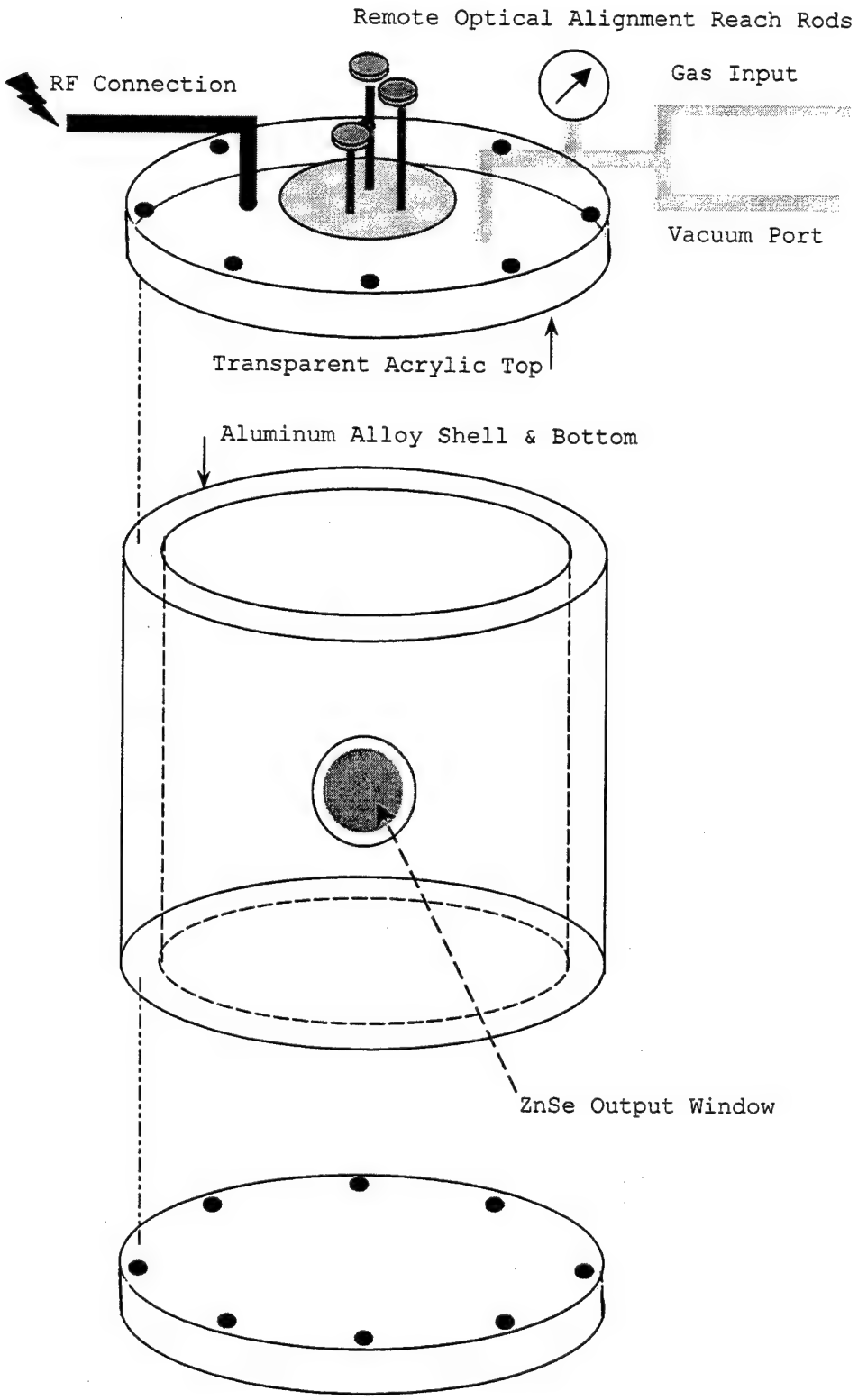

APPENDIX G. VACUUM CHAMBER CRUSH STRENGTH

As discussed in Chapter III, construction of a vacuum chamber to house the laser mechanism and contain the CO_2-N_2-He gas mixture would succeed final assembly and alignment of the optical works and wave guide. The assumption was made that a cylindrical shell design would offer the best overall strength and vacuum tightness (Marks, 1958). The following calculation is offered as a guide for selection of the cylindrical wall thickness to withstand the differential pressure of one atmosphere.

The crushing pressure, W_c, of a cylindrical vessel with flat ends (depicted below) is predicted by the following equation:

$$W_c = KE\left(\frac{t}{D}\right)^3 (psi),$$

where:

t = wall thickness

D = outer diameter of the cylindrical vessel

E = modulus of elasticity (for most aluminum alloys approximately 10^7 psi)

K = dimensionality multiplier, as determined by entering ratios L/R, and D/t into Figure 63, page 5-64, of Marks.

For example, with an internal dimension requirement of 15" across by 16" high, the K factor is approximately 25. Using a 0.5" wall thickness (ideal for machining O-ring grooves), one comes up with a 7,629 psi crush pressure. Clearly, differential pressure (due to vacuum) is not a foreseeable problem for a chamber of this proportion and size.

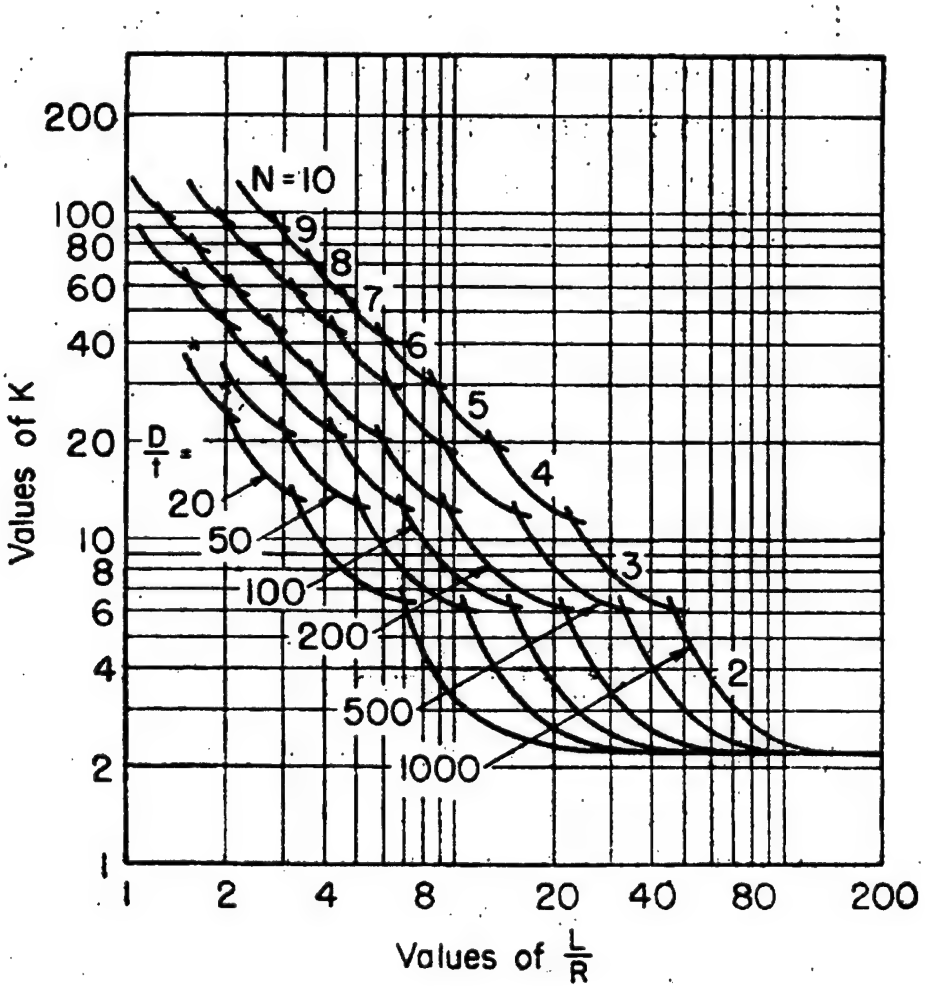

FIG. 63. Radial and end external pressure with fixed edges.

APPENDIX H. INPUTS TO OPTICA SIMULATION

```
Needs["Optica`Optica`"]
```

```
Optica is now loaded.
```

```
inputbeam = Move[CircleOfRays[2], {0, -52, 16}]
```

```
{Ray, Ray, Ray, Ray, Ray, Ray}
```

```
convexmirror = Move[ThinSphericalMirror[200, 50], {100, 0, 0}]
```

```
ThinSphericalMirror
```

```
concavemirror = ThinSphericalMirror[400, 100]
```

```
ThinSphericalMirror
```

```
planemirror = Move[ThinMirror[30], {125, 36, 0.711}]
```

```
ThinMirror
```

LIST OF REFERENCES

Ameritron Corporation, *AL-80B Specifications,* [http://www.ameritron.com/products/ttamps/al80.html], March 1999.

American Radio Relay League, *The ARRL Handbook for Radio Amateurs,* 69th Ed., self-published, 1992.

Beitz, W. and Kuttner, K.-H., *Dubbel Handbook of Mechanical Engineering,* Springer-Verlag, 1994.

Davis, Christopher C., *Lasers and Electro-Optics Fundamentals and Engineering,* Cambridge University Press, 1996.

Day, J. V., *Construction of a Continuous Wave Frequency Modulation Sensitive Laser Radar For Use in Target Identification,* Master's Thesis, Naval Postgraduate School, Monterey, California, March 1997.

Dyer, P. E., "Unstable Resonators," *The Physics and Technology of Laser Resonators,* Institute of Physics Publishing, 1989.

Griffith, G. A., "Transverse RF Plasma Discharge Characterization for CO_2 Waveguide Lasers," *Proceedings of the Society of Photo-Optical Instrumentation Engineers,* Volume 227, pp. 6-11, 1980.

Halliday, D., Resnick, R., and Walker, J., *Fundamentals of Physics Extended, with Modern Physics,* 4th ed., John Wiley & Sons, Inc., 1993.

Hecht, E., *Optics,* 3rd Ed., Addison Wesley Longman, Inc., 1998.

ICOM Incorporated, *HF All Band Transceiver General Coverage Receiver IC-735 Instruction Manual,* ICOM Inc., Japan, 1990.

Lowke, J. J., Phelps, A. V., and Irwin, B. W., "Predicted Electron Transport Coefficients and Operating Characteristics," *Journal of Applied Physics,* Volume 44, Number 10, pp. 4664-4671, October 1973.

Marks, L. S., and Baumeister, T., *Marks' Mechanical Engineers' Handbook, 6th Ed.,* McGraw-Hill Book Company, 1958.

O'Shea, D. C., Callen, R.W., and Rhodes, W.T., *Introduction to Lasers and Their Applications,* Addison-Wesley Publishing Company, 1978.

Patel, C. K. N., "Selective Excitation Through Vibrational Energy Transfer and Optical Maser Action in N_2-$C0_2$," *Physical Review Letters,* Vol. 13(21), pp. 617-619, November, 1964.

Patel, C. K. N., Tien, P. K., and McFee, J. H., "CW High - Power CO_2-N_2-He Laser", *Physical Review Letters,* Vol. 7(11), pp. 290-292, December, 1965.

Parallax Technology, Inc., *Carbon Dioxide Lasers and Carbon Dioxide Laser Tubes,* [http://www.parallax-tech.com/tubes.htm], May, 1999.

Pedrotti, F. L. and Pedrotti, L. S., *Introduction to Optics,* Prentice-Hall, 1987.

Ross, I. E., "CO_2 Waveguide Laser Resonators," *The Physics and Technology of Laser Resonators,* Institute of Physics Publishing, 1989.

Siegman, Anthony E., *An Introduction to Lasers and Masers,* McGraw-Hill Book Company, 1971.

Siegman, Anthony E., *Lasers,* University Science Books, 1986

Simpson, R. E., *Introductory Electronics for Scientists and Engineers,* 2nd Ed., Prentice Hall, 1987.

Svelto, O., *Principles of Lasers,* 4th Ed., Plenum Press, 1982.

Wilson, J. and Hawkes, J., *Optoelectronics, An Introduction,* 3rd Ed., Prentice Hall, 1998.

Witteman, W. J., *The CO_2 Laser,* Springer-Verlag, 1987.

Wojtowich, A. R., *Background Gas Pressure Dependence of Unipolar Arcing on Soda Lima Glass and Plastic Induced by a CO_2 Pulsed Laser,* Master's Thesis, Naval Postgraduate School, Monterey, California, June 1988.

INITIAL DISTRIBUTION LIST

1. Defense Technical Information Center 2
   8725 John J. Kingman Rd., STE 0944
   Ft. Belvoir, Virginia 22060-6218

2. Dudley Knox Library 2
   411 Dyer Road
   Naval Postgraduate School
   Monterey, CA 93944-5101

3. Chairman, (Code PH) 2
   Department of Physics
   Naval Postgraduate School
   Monterey, CA 93943

4. Professor D. Scott Davis (Code PH/Dv) 2
   Naval Postgraduate School
   Monterey, CA 93943

5. Professor Robert C. Harney (Code PH/Ha) 2
   Naval Postgraduate School
   Monterey, CA 93943

6. Lieutenant Erik H. Martin, USN 2
   650 Sloat Avenue, Apartment 14
   Monterey, CA 93940-3650